

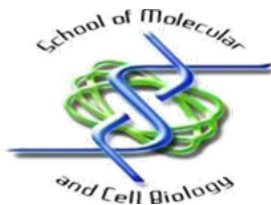


Molecular basis of metabolic reprogramming in innate immune cells: impact of drugs on the mitochondrial function.

Ntombikayise Hendrietta Marcia Xelwa

Student number: 1583242

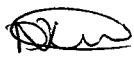
Supervisor: Prof. Monde Ntwasa



A dissertation submitted to the Faculty of Science, University of the Witwatersrand, in fulfilment of the requirements for the degree of Masters of Science.

DECLARATION

I declare that this dissertation is my own, unaided work. It is being submitted for the degree of Master of Science at the University of the Witwatersrand, Johannesburg. It has not been submitted before for any degree or examination at any other University.



Ntombikayise Hendrietta Marcia Xelwa

University of the Witwatersrand

Date: 22 March 2016

ABSTRACT

This study focused on reprogramming of energy metabolism of cancer cells, since most cancer and proliferating cells have been shown to display a metabolic shift by displaying increased dependence on glycolysis and reduced oxidative phosphorylation (OXPHOS) for energy. Dichloroacetate (DCA) and Methyl pyruvate (MP) were used to attempt the reversal of the metabolic program of THP-1 cells. Flow cytometry was used to determine the mode of cell death and to analyse the changes in cell cycle.

In this study, an overexpression of TLR4 was observed in THP-1 cells treated with 5ng/ml of lipopolysaccharides (LPS). Further analysis of cell death showed that MP and DCA-treated cells resulted to minimal induction of apoptotic cell death. This suggests that the 2 drugs (MP and DCA) cause cell death via apoptosis. Furthermore, LPS treated cells (infected cancer cells) showed an increase in glycolysis (Warburg effect). This study has shown that indeed treatment with drugs such as MP and DCA was effective in reversing the glycolytic phenotype of THP-1 cells, resulting in cell death via apoptosis by boosting OXPHOS.

ACKNOWLEDGEMENTS

My sincere gratitude goes to my supervisor Prof Monde Ntwasa for taking me in as his student. Thank you for the great advice and encouragement.

My parents, Mr and Mrs Xelwa. Thank you for believing in me, encouraging and supporting me every step of the way.

My husband Siyabonga Mhlambi for his love, encouragement and support, you are my pillar of strength.

All my siblings for always being there for me.

I would like to convey my great appreciation to my mentor Dr. Ekene Nweke for his sincere advice, support and constant encouragement.

Fly lab colleagues; Philemon Ubanako, Zanele Nsingwane, Umar-Faruq Cajee, Charmy Twala and Bernice Monchusi.

I would also like to thank National Research Foundation (NRF) for their financial support.

QUOTATION

It always seems impossible until it's done.

Nelson Mandela.

RESEARCH OUTPUTS

Poster presentation

Ntombikayise Xelwa and Prof. Monde Ntwasa. Molecular basis of metabolic reprogramming in innate immune cells: impact of drugs on the mitochondrial function. Wits Cancer Research Symposium, University of the Witwatersrand, Johannesburg, 09 February 2017.

Poster presentation

Ntombikayise Xelwa and Prof. Monde Ntwasa. Molecular basis of metabolic reprogramming in innate immune cells: impact of drugs on the mitochondrial function. Wits 8th cross-Faculty graduate symposium. University of the Witwatersrand, Johannesburg, 25 October 2017. Wits 8th cross faculty graduate symposium showcasing postgraduate research. University of the Witwatersrand, Johannesburg, 25 October 2017.

Poster presentation

Ntombikayise Xelwa and Prof. Monde Ntwasa. Metabolic reprogramming in innate immune cells: impact of drugs on the mitochondrial function. Annual Molecular Biosciences Research Thrust (MBRT) Research Day 2017, University of the Witwatersrand, Johannesburg 30 November 2017.

TABLE OF CONTENTS

| | |
|--|------|
| DECLARATION | i |
| ABSTRACT | ii |
| ACKNOWLEDGEMENTS | iii |
| QUOTATION | iv |
| RESEARCH OUTPUTS | v |
| LIST OF FIGURES | viii |
| LIST OF ABBREVIATIONS | x |
| CHAPTER 1: INTRODUCTION | 1 |
| 1.1 Overview of cancer | 1 |
| 1.2 Metabolic reprogramming in cancer and immune cells | 2 |
| 1.3 Cellular respiration | 3 |
| 1.4 Hypoxia and HIF-1α role in immunity, carcinogenesis and metabolism | 4 |
| 1.5 Lipopolysaccharide (LPS) and neutralization thereof by Polymyxin B (PmB) | 5 |
| 1.6 TLR signalling pathway | 7 |
| 1.7 Association of cancer and infection | 8 |
| 1.8 Mechanisms used by which LPS promotes Warburg metabolism in innate immune cells .. | 9 |
| 1.8.1 Nitric oxide (NO) and metabolic changes in macrophages and Dendritic cells | 9 |
| 1.8.2 Hypoxia-inducible factor-1α (HIF-1α) and glycolysis | 9 |
| 1.8.3 AMPK and activation of macrophages and DCs | 10 |
| 1.9 Apoptosis | 10 |
| 1.9.1 Morphology of Apoptotic Cells | 11 |
| 1.9.2 Apoptotic Pathways | 11 |
| 1.10 Cell cycle | 12 |
| 1.11 Reversal of metabolic reprogramming | 13 |
| 1.12 Justification of study | 16 |
| 1.13 Aim | 17 |
| 1.14 Objectives | 17 |
| CHAPTER 2: MATERIALS AND METHODS | 19 |
| 2.1 Materials | 19 |
| 2.2 Methods | 19 |
| 2.2.1 An overview of the methods | 20 |
| 2.2.2 Cell line | 21 |
| 2.2.3 Cell culturing routine and treatment | 21 |
| 2.2.4 Cell counting and viability determination | 21 |
| 2.2.5 Cell cryopreservation and recovery | 22 |

| | |
|--|-----------|
| 2.2.6 RNA extraction using TRIzol method..... | 22 |
| 2.2.7 Complementary DNA synthesis (Reverse Transcription) | 23 |
| 2.2.8 Polymerase Chain Reaction (PCR)..... | 24 |
| 2.2.9 Agarose gel electrophoresis | 25 |
| 2.2.10 Flow cytometry | 26 |
| 2.2.11 Glycolysis and OXPHOS assays | 28 |
| 2.3 Image and statistical analysis..... | 29 |
| CHAPTER 3: RESULTS | 30 |
| 3.1 Overview | 30 |
| 3.2 Expression of TLR 4 in THP-1 cells using RT-PCR..... | 30 |
| 3.3 Cell cycle analysis of THP-1 human monocytic cells following various treatments in a time-dependant analyses. | 31 |
| 3.3.1 Distribution of cells in sub G0/G1 phase after treatment..... | 34 |
| 3.4 Apoptosis induction following various treatments..... | 37 |
| 3.5 Glycolysis and OXPHOS assays following treatment with drugs that reverse the Warburg effect. | 39 |
| CHAPTER 4: DISCUSSION | 42 |
| 4.1. TLR 4 is overexpressed in untreated THP-1 cells compared to the LPS-treated cells..... | 42 |
| 4.2 Introduction of exogenous pyruvate or augmenting endogenous pyruvate induces apoptosis | 44 |
| 4.3 Exogenous and endogenous pyruvate reverse the metabolic reprogramming in THP-1 cells (Warburg effect) | 45 |
| 4.4 Conclusion | 46 |
| 4.5 Future studies | 47 |
| REFERENCES..... | 48 |
| APPENDIX A: CHEMICALS AND REAGENTS..... | 57 |
| APPENDIX B: LABORATORY EQUIPMENT..... | 58 |
| APPENDIX C: KITS | 59 |
| APPENDIX D: BUFFERS | 59 |
| APPENDIX E: CELL CYCLE RAW DATA GENERATED USING BD ACCURI..... | 60 |
| APPENDIX F: FLOW CYTOMETRY OBTAINED APOPTOSIS RESULTS, FOLLOWING VARIOUS TREATMENTS | 66 |
| APPENDIX G: GLYCOLYSIS RESULTS AND STANDARD CURVE FOLLOWING 24 HOURS OF TREATMENT | 72 |
| APPENDIX H: OXPHOS RESULTS FOLLOWING 24 HOURS OF TREATMENT..... | 73 |

LIST OF FIGURES

| | |
|--|----|
| Figure 1.2: Schematic overview of the TLR signalling pathway. | 8 |
| Figure 1.3: Schematic representation of the cell cycle | 13 |
| Figure 1.5: A simplified diagrammatic representation of the metabolic pathways (Glycolysis and OXPPOS)..... | 17 |
| Figure 2.1 Flowchart diagram showing methods used in study. | 20 |
| Figure 3.2: The effects of various drugs treatments on the cell cycle progression in THP-1 cells at various time intervals (6, 12,18, and 24 hours). | 33 |
| Figure 3.4: Cell cycle analysis in THP-1 human monocytic cells. | 35 |
| Figure 3.5: Cell cycle analysis in THP-1 human monocytic cells. | 36 |
| Figure 3.6: Cell cycle analysis in THP-1 human monocytic cells. | 36 |
| Figure 3.7: Effects of various treatments on inducing apoptosis in THP-1 cells following 24 hours of treatment..... | 38 |
| Figure 3.8: Statistical analysis of flow cytometry results-obtained a) apoptosis and b) necrosis (%) in THP-1 cells following 24 hours of treatment. | 39 |
| Figure 3.9 Glycolysis was analysed in THP-1 cells using the Cayman’s dual assay kit system which relies on measurement of lactate (indication of the glycolytic activity) in 96 well plates following various treatments for 24 hours..... | 41 |
| Figure 3.10: OXPPOS was analysed in THP-1 cells using the Cayman’s dual assay kit system which relies on measurement of quenched oxygen (indication of OXPPOS activity) in 96 well plates following various treatments for 24 hours. | 41 |
| Figure A1: Standard curve for the L-Lactate concentrations obtained from the L-lactate concentrations (orange) and glycolysis assay treatments (blue). | 72 |

LIST OF TABLES

| | |
|---|----|
| Table 2.1: cDNA synthesis reagents | 24 |
| Table 2.2: PCR cycling conditions and time spent per cycle..... | 24 |
| Table 2.3: PCR 50 µl reaction mixture | 25 |
| Table 2.4: Primers used for TLR 4 mRNA expression..... | 25 |

LIST OF ABBREVIATIONS

| | |
|----------------|--|
| Apaf-1 | Apoptosis protease-activating factor-1 |
| ATP | Adenine triphosphate |
| Bad | Bcl-xL/Bcl-2-associated death protein |
| Bax | Bcl-2-associated death protein |
| Bid | B cell leukaemia lymphoma-2 |
| Cdk | Cyclin-D dependent kinase |
| cDNA | Complementary DNA |
| DAMP | Damage associated molecular pattern |
| DCA | Dichloroacetate |
| DMSO | Dimethylsulfoxide |
| DNA | Deoxyribonucleic acid |
| <i>E. coli</i> | <i>Escherichia coli</i> |
| FBS | Fetal bovine serum |
| GAPDH | Glyceraldehyde 3-phosphate dehydrogenase |
| GLUT | Glucose transporter |
| HIF | Hypoxia inducible factor |
| LBP | LPS-binding protein |
| LPS | Lipopolysaccharide |
| MP | Methyl pyruvate |
| mM | Millimolar |
| mRNA | Messenger ribonucleic acid |
| NF- κ B | Nuclear factor κ B |
| ng | Nano grams |
| NLR | NOD-like receptor |

| | |
|--------------|---|
| NO | Nitric oxide |
| OXPPOS | Oxidative phosphorylation |
| PAMP | Pathogen associated molecular pattern |
| PBS | Phosphate buffered saline |
| PCR | Polymerase chain reaction |
| PDH | Pyruvate dehydrogenase |
| PDK | Pyruvate dehydrogenase kinase |
| PmB | Polymyxin B |
| PI | Propidium iodide |
| PRR | Pathogen recognition receptor |
| PS | Phosphatidyl serine |
| RLR | RIG-like receptor |
| ROS | Reactive oxygen species |
| RT-PCR | Reverse transcription polymerase chain reaction |
| RNA | Ribonucleic acid |
| TCA | Tricarboxylic acid |
| TLR | Toll like receptor |
| TNF | Tumour necrosis factor |
| V | Volts |
| α | Alpha |
| κ | Kappa |
| μ l | Micro litre |
| % | Percentage |
| $^{\circ}$ C | Degrees Celsius |

CHAPTER 1: INTRODUCTION

1.1 Overview of cancer

According to statistics from GLOBOCAN, cancer is a growing public health problem (International Agency for Research on Cancer and World Health Organization 2014), with more than 14 million cases newly diagnosed cancer patients in 2012 and about 8 million of those patients lived in the less developed regions of the world. Statistics for the year 2012 indicate that cancer killed slightly more than 8 million people and 5.3 million cases were reported in less developed regions. It is estimated that nearly 50% of all new cancer patients will die within 12 months of diagnosis as the five-year survival rates for all cancers in both developing and developed countries have been found to range from 30 to 60% (Kaur and Mohanti, 2011).

Cancer has been defined as a cell growth disorder, that can be characterised by proliferation of genetically dysfunctional cells (Raven and Johnson, 1996). When cells continue to replicate in an uncontrolled manner, they lead to a cluster of cells known as a tumour or a neoplasm. When the neoplastic cells remain clustered together, they are found to be non-cancerous and can be removed with surgery. Cancerous cells become harmful when they invade the surrounding tissue and break away from the tumour. They enter the blood or lymph vessels and form secondary tumours known as metastases in other parts of the body. Cancers are classified according to the tissue and cell type from which they develop. Carcinomas develop from epithelial cells, whereas cancers of the connective tissue or muscle cells are referred to as sarcomas. Other cancers arising from haemopoietic cells, known as leukaemia, and nervous tissue do not fall into these categories (Raven and Johnson, 1996).

Leukemia is a type of cancer reported to arise from the dysfunction of the hematopoietic cells in bone marrow, arising from inequalities of intracellular DNA molecules. The excessive formation of immature leucocytes obstructs numerous functions of the bone marrow and as a result the count of normal blood cells decreases significantly. Leukemia cancer was found to be the most prevalent

while its mortality as a malignant disorder ranks first when compared to other pediatric cancers. Leukemia cells can migrate to other parts of the body including central nervous system, spleen, lymph nodes, liver (Mardiros *et al.*, 2013). Leukemia can be classified into four major classes; lymphoblastic leukemia, chronic lymphocytic leukemia, chronic myeloid leukemia and acute myeloid leukemia (Vardiman *et al.*, 2009). Current treatment for leukemia involves therapeutic options such as chemotherapy, radiotherapy or combination of both. In some cases, bone marrow and targeted therapy is required. Most cases of leukemia are treated using chemotherapeutic drugs that are combined into a multidrug dose therapy, treatment has proven unsuccessful (Hoffbrand *et al.*, 2006). The drug resistance indicates the non-susceptible nature of leukemia cells towards chemotherapeutic drugs (Badura *et al.*, 2013). Taken together, targeting the energy metabolism of cancer cells might provide a promising avenue for cancer therapy.

Cancer cells display an increased use of glucose via glycolysis as a cellular resource, (Warburg effect). In contrary to normal cells, cancer cells often display dysregulated metabolism and take advantage of the abundant resources available within the body. Intermediates produced through glycolysis are diverted to biosynthetic pathways that are necessary to produce the building blocks to keep up with these highly proliferative cells. Carbon from glucose is used for the synthesis of nucleotides and amino acids. These metabolic changes observed in cancer allow readily available resources to be converted into biomass in an efficient manner. This metabolic shift releases cells from the typical restraints on growth, and provides a potential way to distinguish them from healthy cells and this allows for treatments that may be selective for cancerous cells.

1.2 Metabolic reprogramming in cancer and immune cells

In non-proliferative cells, glucose is metabolized to pyruvate, an end product of glycolysis that is converted to Acetyl-CoA. Acetyl-CoA then enters the TCA cycle and further down into the electron transport chain (Warburg *et al.*, 1927). Within the TCA cycle and OXPHOS, the acetyl CoA is oxidized to carbon dioxide and water, generating 36 ATP molecules. In contrast, most cancer and proliferating cells have been shown to display a metabolic shift by displaying

dependence on glycolysis as opposed to oxidative phosphorylation (OXPHOS) for energy. Cancer cells depend primarily on the glycolytic pathway for production of energy in the form of ATP and for the synthesis of metabolic intermediates to shunt into biosynthetic pathways. This phenomenon is commonly known as the Warburg effect (Warburg, 1956). They utilize multiple mechanisms that help them reprogram their metabolism. Cancer cells reprogram their metabolic pathways to ensure ATP is readily available for nutrient synthesis and proliferation. Although glycolysis only yields 2 ATPs while OXPHOS 36 ATPs, cancer cells still prefer the glycolytic pathway as it is faster, giving them a constant supply of ATP. Constantly proliferating cells like cancers require bioenergetic and biosynthetic activities, which are redirected towards nucleic acids, fatty acids and amino acids production to ensure the cell proliferation (DeBerardinis *et al.* 2008). The metabolic switch observed in cancer cells is facilitated by oncogenes and tumour suppressors (Vogelstein and Kinzler, 2004). This is achieved by maintaining high rates of glycolysis, slowing glycolytic end-product entry into OXPHOS and utilizing TCA intermediates for biosynthetic precursors.

Upon stimulation of the innate immune cells by agonists such as Lipopolysaccharide (LPS), innate immune cells also rewire their metabolism in a manner similar to that observed in cancer cells. Innate immune cells display a shift in metabolism by showing an increase in glycolysis and decrease in OXPHOS (Krawczyk *et al.*, 2010; West *et al.*, 2011).

1.3 Cellular respiration

Glycolysis

Glycolysis involves several enzymes in the 10-step reaction, where some of the glycolytic intermediates serve as carbon sources for the synthesis of macromolecules precursors. During glycolysis, glucose is transported by glucose transporters (GLUT) into the cell. Inside the cell, glucose completely oxidized in order to produce energy in the form of adenine triphosphate (ATP). During glycolysis (which occurs in the cytoplasm of the cell), glucose (a six-carbon molecule) is converted into two 3-carbon molecules of pyruvate and ATP is formed. This is a ten-step reaction that involves multiple enzymes. Two ATP

molecules, two pyruvate molecules and two electron carrying molecules of NADH are produced per glucose molecule (Figure 1.6).

Tricarboxylic acid cycle (TCA)

Each pyruvate molecule is converted to Acetyl CoA, which then moves into the mitochondria. Acetyl CoA binds to oxaloacetate through a series of enzymic reaction. This yields the production of NADH, FADH, ATP and carbon dioxide (Figure 1.6).

Electron transport chain

Occurs in the mitochondria, which is responsible for providing the majority of cellular ATP through a series of membrane-bound carriers that pass electrons from one to another (Boneh, 2006). OXPHOS is comprised of five protein complexes that located in the inner mitochondrial membrane. These complexes (I-IV) are responsible for transferring electrons. This energy transfer allows complexes to pump electrons throughout the inter mitochondrial membrane space, leading to the generation of a proton gradient. The proton gradient is used by an enzyme called ATP synthase to mechanically generate ATP (Collins *et al.*, 2002).

Reactive oxygen species

Reactive oxygen species (ROS) must be present within a certain range for a normal cellular function to occur, therefore it is important that production of ROS is controlled. ROS include a variety of molecules and free radicals that are derived from molecular oxygen such as superoxide anion and peroxide radical. Non-radical species such as hydrogen peroxide (H₂O₂) are also found to be reactive (Balaban *et al.*, 2005). ROS can be produced by NADH oxidase, as well as by the mitochondria as a by-product of OXPHOS. Production of ROS can also be triggered by external agents. Excessive production of ROS can be harmful to human cells as they induce DNA damage (Kowaltowski *et al.*, 2009).

1.4 Hypoxia and HIF-1 α role in immunity, carcinogenesis and metabolism

Hypoxia, is a characteristic of many cancer cells and occurs because of enhanced cell proliferation. It has been shown to be involved in metabolic reprogramming

in some cancer cell lines. For example, the contribution of OXPHOS to ATP production by HeLa and MCF cells drops by 50% when the cells are exposed to hypoxic environments (Rodríguez-Enríquez *et al.*, 2010). However, other mechanisms have been found to be involved in metabolic reprogramming of cancer cells in normoxic microenvironments. This observation was made in lung cancers which are found in microenvironments of high oxygen tension but still display high glycolysis (Elstrom *et al.*, 2004; Christofk *et al.*, 2008), which confirms that metabolic reprogramming can be triggered by hypoxia-independent mechanisms. Lipopolysaccharides (LPS) from gram negative bacteria are also known to activate the expression of HIF-1 α in normoxic microenvironments. In a recent study, LPS was shown to induce the expression of HIF-1 α in a translation-dependent manner, mediated by TLR4 and accompanied by an increased expression of glycolytic genes such as GLUT1, lactate dehydrogenase and phosphoglycerate kinase (Jantsch *et al.*, 2008). In lung cancer cells, HIF-1 α drives metabolic reprogramming, decreases ROS levels and eases metastatic colonization (Zhao *et al.*, 2014). This serves, at least in part as one of the mechanisms by which metabolic reprogramming occurs in activated innate immune cells and in tumour cells.

1.5 Lipopolysaccharide (LPS) and neutralization thereof by Polymyxin B (PmB)

LPS is a layer that is found on the cell wall of Gram-negative bacteria. It consists of two main parts namely; a polysaccharide part and a lipid part (Figure 1.1). The lipid A structure is the one which is responsible for the immune activation of LPS. The LPS molecule differ between different gram-negative bacteria and this is why some bacteria may be more immunogenic than others (Zughaier *et al.*, 2005). In innate immune cells (upon infection by LPS), free LPS is bound by LPS binding protein (LBP) and CD14 and transported to the cell membrane of immune cells, such as antigen presenting cells. The complex is recognised by TLR4/MD2 and initiates cellular signalling. Lipopolysaccharide is a potent inducer of pro-inflammatory responses. Activation of cells with LPS has led to the secretion of several cytokines and chemokines (Corinti *et al.*, 2001; Verhasselt *et al.*, 1997). LPS was used to mimic infection.

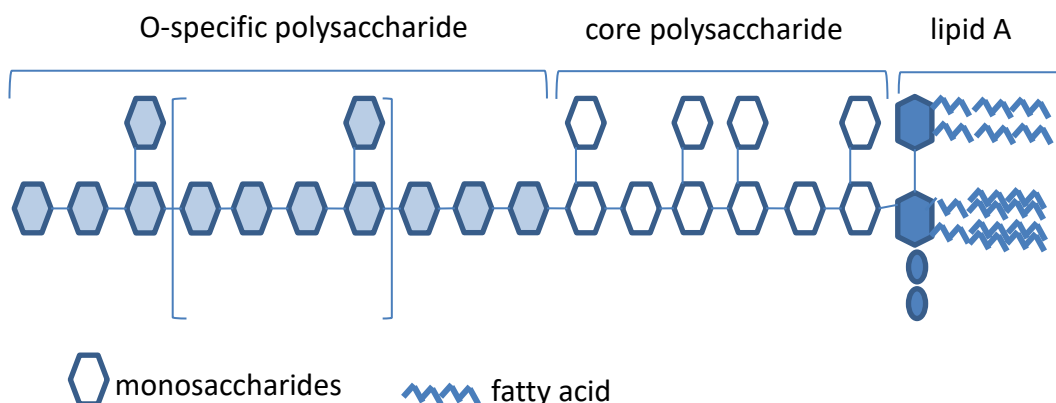


Figure 1.1: A simplified LPS structure. Schematic diagram showing the lipid A and polysaccharide portions of LPS. An illustration of the three different portions of the LPS molecule.

Antibiotics are naturally found in biological materials in very small quantities. They have been evolving from natural sources and many efforts are being done to synthesize and develop their relatives holding specific structures. These structures are different in their mechanisms of action. Polymyxin B (PmB) was used in this project to neutralize LPS by blocking its activity. Polymyxins are antibiotics that actively act against gram negative bacteria. The generic name of polymyxins was derived from bacteria *Bacillus polymyxa* (Moyer *et al.*, 1953). Polymyxins B is a member of a large class of five polymyxins isolated by *Bacillus* species. Other polymyxins include A, C, D and E, but the only members of class to achieve clinical use were from polymyxin B and E because other polymyxins have shown to display high toxicity (Falagas *et al.*, 2005). Polymyxins are amphipathic antibiotics that act on the external and cytoplasmic membranes. They work through a variety of mechanisms including binding to cell envelope components such as phospholipids and LPS and thus interferes with cell processes such as causing displacement of calcium and magnesium ions, which act as membrane stabilizers, this leads to the rupture of the cell membrane which in turn results in loss of cellular contents, thus killing bacteria (Storm *et al.*, 1977). The binding and inactivation capacity of LPS, has been found to be effective in reducing the inflammatory stimulus induced by LPS (Cooperstock, 1974). Removal of LPS and inflammatory mediators with polymyxin B, have been proven successful (Shoji, 2003; Vincent *et al.*, 2005).

1.6 TLR signalling pathway

The innate immune system is made of Pattern recognition receptors (PRR) which are structures that are activated following recognition of pathogen associated molecular patterns (PAMPs). PAMPs are unique structures from bacteria, viruses, parasites and fungi and damage associated molecular patterns (DAMPs) are released endogenously by necrotic cells (Park *et al.*, 2006; Raucchi *et al.*, 2007; Curtin *et al.*, 2009). PRRs are expressed on various cells of the immune system such as monocytes, macrophages, dendritic cells, NK cells, mucosal epithelial and endothelial cells (He *et al.*, 2007). There are several families of PRRs, but the best characterized are the NOD-like receptor (NLR), RIG-1-like receptor (RLR) and Toll-like receptor (TLR) (Liu, 2008). NLRs belong to a large family of cytosolic receptors. They are present inside the cells where they sense intracellular bacterial invasion. The best studied NLRs are NOD1 and NOD 2, which recognize peptidoglycan of bacterial cell walls (Creagh and O'Neill, 2006). RLRs are soluble pathogen recognition receptors that reside in the cytosol of the cells where they act as sensors of viral infections (Creagh and O'Neill, 2006).

This study focused on Toll-like receptors (particularly TLR 4). A family of evolutionary conserved PRRs (Roach *et al.*, 2005), was first identified in the fruit fly *Drosophila*, and found to be involved in embryogenesis as well as in protection against fungi infection (Lemaitre *et al.*, 1996). Thus far, 11 TLRs have been discovered in humans with the first TLR to be discovered being TLR 4 (Medzhitov *et al.*, 1997). TLRs are classified as type I membrane proteins that have an ectodomain with leucine rich repeats and a conserved Toll/Interleukin-1 (TIR) receptor domain in the cytoplasmic region (O'Neill *et al.*, 2003; Takeda and Akira, 2005). In response to their corresponding ligands (such as LPS), TLRs initiate a signalling cascade that leads to the expression of transcription factors such as nuclear factor- κ B (NF κ B). NF κ B initiates the expression of pro-inflammatory cytokines and chemokines (Takeda and Akira, 2004). In innate immune cells (upon infection by LPS), free LPS is bound by LPS binding protein (LBP) and CD14 which is then transported to the cell membrane of immune cells. The complex is recognised by TLR4/MD2 and initiates cellular signalling (figure 1.2).

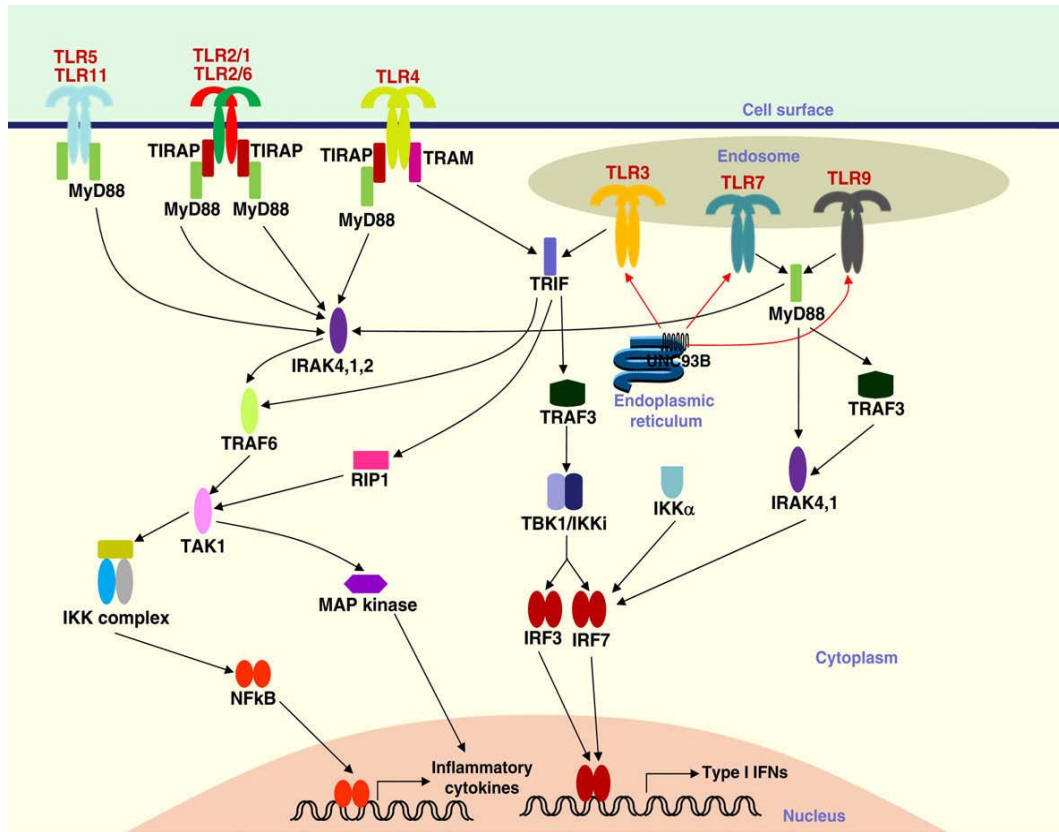


Figure 1.2: Schematic overview of the TLR signalling pathway. Upon stimulation by its specific ligand. TLRs recruit adaptor proteins called MyD88 (myeloid differentiation factor 88), MAL (MYD88-adaptor-like protein). This leads to the phosphorylation of (Inhibitor κ B), which renders NF κ B free from its inhibitor. NF κ B then translocates to the nucleus where it activates inflammatory cytokines and chemokines (Himanshu et al., 2009).

1.7 Association of cancer and infection

The link between cancer and inflammation was made following observations that cancer deaths have been associated with infections and chronic inflammation (Balkwill and Mantovani, 2001). These infections trigger chronic inflammation which is an important factor that contribute in carcinogenesis (Parkin, 2006). Chronic inflammation has been associated with certain types of cancer. Examples of such includes infection with *Helicobacter pylori* which has been associated with gastric cancer, and inflammatory bowel disease has been associated with colon cancer (Koehne and Dubois, 2004; Flossmann and Rothwell, 2007). The hallmarks of cancer-related inflammation include the presence of inflammatory cells and inflammatory mediators (such as chemokines and cytokines) in tumor

tissues similar to that seen in chronic inflammatory responses and tissue repair (Borrello, 2005). Toll-like receptor activation by PAMPs has been shown to be involved in cancer progression (Huang *et al.*, 2005). Upon infection, cells such as macrophages and dendritic cells reprogram themselves in the same manner as cancer cells. This metabolic switch is facilitated by interleukin 10 (IL-10) (Krawczyk *et al.*, 2010). This creates a link between TLR-signalling and carcinogenesis.

1.8 Mechanisms used by which LPS promotes Warburg metabolism in innate immune cells

The Warburg effect is important in understanding metabolic changes occurring in innate immune cells upon activation. To understand the metabolic changes occurring in the innate immune cells upon infection, it is important to study the Warburg effect.

1.8.1 Nitric oxide (NO) and metabolic changes in macrophages and Dendritic cells

Upon stimulation of innate immune cells with its agonist LPS, decreased levels of OXPHOS and increased levels of glycolysis is observed. Stimulation of these cells with LPS have shown to increase the expression of inducible nitric oxide synthase (iNOS), which generates nitric oxide (NO), these are reactive nitrogen species that can inhibit mitochondrial respiration (Lorsbach *et al.*, 1993; Lu *et al.*, 1996). Nitric oxide is known to inhibit OXPHOS by nitrosylating iron-sulphur proteins such as cytochrome C oxidase and Complex I in the electron transport chain, this decreases the activity of the electron transport chain (Drapier and Hibbs, 1988; Cleeter *et al.*, 1994).

1.8.2 Hypoxia-inducible factor-1 α (HIF-1 α) and glycolysis

Many cancer cells are exposed to hypoxic conditions where they cannot rely on OXPHOS and must modify their metabolism to survive under conditions of reduced oxygen tension. HIF-1 α is a transcription factor that promotes the switch to glycolysis and this allows cancer cells to continue producing ATP under limited oxygen conditions (Denko, 2008). Under these circumstances pyruvate, an end product of glycolysis, does not feed into the TCA cycle to boost OXPHOS, but is instead metabolized to lactate. HIF-1 α is responsible for this metabolic switch by

binding to hypoxia response elements in target genes (Semenza *et al.*, 1991; Mole *et al.*, 2009). HIF-1 α promotes glycolysis by binding to glucose transporter GLUT1, which increases the entry of glucose into the cell (Chen *et al.*, 2001). HIF-1 α also increases the expression of glycolytic enzymes such as lactate dehydrogenase (Semenza *et al.*, 1996), this enzyme is responsible for catalysing pyruvate into lactate, thereby limiting the entry of pyruvate into the TCA cycle. Another enzyme that promotes glycolysis is pyruvate dehydrogenase kinase which inhibits pyruvate dehydrogenase (Kim *et al.*, 2006; Papandreou *et al.*, 2006). This leads to increased levels of glycolysis and decreased levels of OXPHOS.

1.8.3 AMPK and activation of macrophages and DCs

The principal enzymatic activity of AMP-activated protein kinase (AMPK) is to sense energy in macrophages and when stimulated by LPS, the activity of this enzyme is decreased (Sag *et al.*, 2008). AMPK has been shown to be active when the cellular energy is low and induces the expression of proteins involved in OXPHOS. The main function is to conserve energy when it is limited by inhibiting anabolic pathways, such as gluconeogenesis, and promoting catabolic pathways, such as β -oxidation of fatty acids. Therefore, decreasing the enzymatic activity of AMPK increases glycolysis while reducing OXPHOS (Vats *et al.*, 2006).

1.9 Apoptosis

Apoptosis was first described by Kerr, Wyllie and Currie in 1972 as a programmed cell death. This is a genetically controlled form of cell death which plays an important role in normal tissue development. Apoptosis is involved in organogenesis, tissue homeostasis and remodelling (McKenna, 1996). The process of apoptosis has been described as an active bio-energy saving cell-elimination mechanism, which removes aged, unwanted or damaged cells. The cellular contents of these cells are phagocytosed by adjacent cells or macrophages and these cells are recycled (Vermees *et al.*, 1997). Cancer cells can avoid apoptosis and they continue to proliferate, therefore it is important to use drugs that induce apoptosis (Debatin, 2004).

1.9.1 Morphology of Apoptotic Cells

Apoptosis is characterised by several distinct morphological changes, including blebbing, fragmentation of the nucleus, cell shrinkage, DNA fragmentation and lastly cell death (Ouyang *et al.*, 2012). The cytoplasm and nucleus become condensed and the chromatin aggregates along the nuclear membrane. Degradation at the inter nucleosomal sites of the cellular DNA leads to fragments and results in the segmented appearance of the nucleus. The membrane appears to be blebbing as the endoplasmic reticulum is transformed. The cell membrane becomes rigid due to the cross-linking of the membrane proteins before the cell is broken apart into small vesicles called apoptotic bodies. These remain in the extracellular space until they are phagocytosed by the neighbouring cells or by the macrophages (Vermes *et al.*, 1997; Story and Kodym, 1998; Corfe, 2002; Golstein *et al.*, 2003). No damage to the surrounding cells occurs, and no inflammatory response is initiated during apoptosis. This change of the cell membrane and the altering of the surface hydrophobicity and charge may be recognised by the macrophages (Vermes *et al.*, 1997; Corfe, 2002).

1.9.2 Apoptotic Pathways

There are two main pathways that control apoptosis, namely the death receptor pathway (extrinsic) and mitochondrial pathway (intrinsic), (Wen *et al.*, 2012). The presentation of an appropriate ligand for a death receptor causes these to form a multi-protein complex called the death-induced signalling complex. This complex triggers the direct activation of caspase-8, which belongs to a proteinase family known as the caspases. The caspases are thought to be activated and specifically during apoptosis. Certain caspases can auto-activate and can then activate other caspases and a variety of other cellular substrates. These are involved in the breaking down and packaging of the cellular components into apoptotic bodies (Vermes *et al.*, 1997; Green and Reed, 1998, Thornberry and Lazenbnik, 1998; Li and Yuan, 1999; Adrain and Martin, 2001).

The second pathway involves intracellular signalling that targets the mitochondria, this pathway is regulated by a family of the Bcl-2 protein family. These include proapoptotic Bak and Bax, and the anti-apoptotic Bcl-xL and Bcl-2 proteins. Bcl-xL and Bcl-2 may also be present in the endoplasmic reticulum and

the nuclear membrane in some cell types, and often Bax is found in the cytosol. Once apoptosis is stimulated, Bax is recruited to the mitochondria where it binds to Bak. This complex forms pores in the membrane, allowing the release of cytochrome c from the outer mitochondrial membrane and into the cytoplasm and the loss of mitochondrial membrane potential. An apoptosome body is formed, which is a protein complex consisting of pro-caspase 9 and APAF-1, then binds with the released cytochrome c. This leads to the activation of caspase-9, which in turn cleaves into active caspase-3 which is responsible for inducing apoptosis (Vermes *et al.*, 1997; Green and Reed, 1998, Thornberry and Lazenbnik, 1998; Li and Yuan, 1999; Adrian and Martin, 2001; Pommier *et al.*, 2004).

1.10 Cell cycle

For an organism to grow and function properly, the cell cycle has to be completed. Cell cycle consists of four phases, namely the S-phase whereby the DNA is replicated (figure 1.3). The M-phase, two identical chromosomes are distributed evenly into two daughter cells (Sherr, 1996). During the G1 phase, preparations of DNA synthesis occurs and lastly the G2 phase prepares for cell division or mitosis (Vermeulen *et al.*, 2003). Cells in the G0 phase are in a quiescent state, and these cells do not divide even though they are still active (Park and Lee, 2003).

One of the hallmarks of cancer development is the ability of these cells to proliferate uncontrollably and cancer cells show mutated genes which play a role in the regulation of the cell cycle (Sherr, 1996). p53 is a tumour suppressor protein and p16 is a tumour suppressor gene, both of which control the cell cycle (Jacks and Weinberg, 1998).

Cyclin-dependent kinases (CDK's) are proteins that drive the progression of the cell through the stages of the cell cycle (Israels *et al.*, 2000). Activities of the CDKs are regulated by cyclins and cyclin dependent kinase (CAK), which is a serine/threonine kinase (Nigg, 1996). The cell cycle is regulated by many genes and these genes have also been found to control apoptosis (Alenzi, 2004). p53 plays an important role in the relationship between apoptotic cell death and cellular proliferation (Haupt *et al.*, 2003), whose role includes the maintenance of genome integrity in the G1-S and G2-M checkpoints of the cell cycle. This is

done to detect any DNA damage, thus prevents the progression of aberrant cells through the cell cycle (Jin and Levine, 2001). When DNA damage is found during the cell cycle checkpoints, regulatory signals that induce cyclin dependent kinase inhibitors (CKIs) which stops the cells cycle and repairs the DNA damage (Sherr, 2000). Mutations in p53 prevents proper functioning of the G1-S and G2-M checkpoints, which in turn allows the damaged cells to survive and proliferate uncontrollably, this then leads to the promotion of cellular growth (Jin and Levine, 2001).

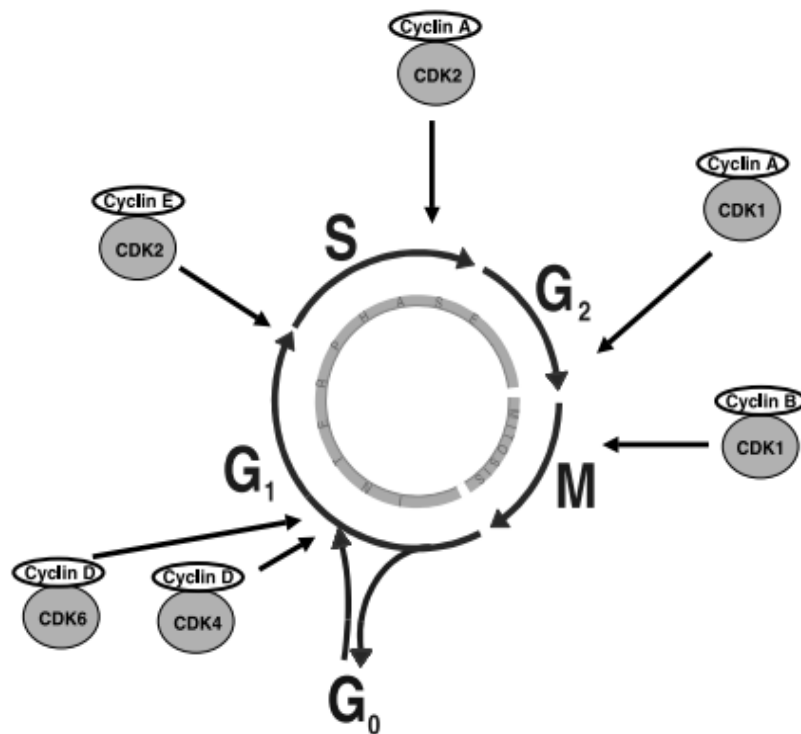


Figure 1.3: Schematic representation of the cell cycle phases (G₀, G₁, S and G₂ and M) (Vermeulen et al. 2003).

1.11 Reversal of metabolic reprogramming

Cancer cells reprogram their metabolism consequently enabling their proliferation and migration, thus, reversal of their metabolic processes might be toxic to them and inhibit growth. In this study, drugs such as dichloroacetate and methyl pyruvate were utilized to reverse the Warburg effect. These drugs are known to function in reversing the metabolic reprogramming in cancer cells.

Dichloroacetate (DCA)

Preference of cancer cells to utilize increased levels of glycolysis as a primary metabolic pathway for the generation of ATP and reduced OXPHOS levels (Warburg effect) has created opportunities for targeting the Warburg effect as a potential therapeutic target in cancer therapy. Studies by Bonnet *et al.*, 2007; Michelakis *et al.*, 2008 have shown that reversing the Warburg effect in cancer cells may result in the induction of apoptosis in cancer cells. Cancer cells rewire their metabolism by showing less dependence on OXPHOS, as it gives cancer cells the unique ability to avoid apoptotic effects in the mitochondria.

DCA is a water-soluble agent with 100% bioavailability when administered orally. This is the case because DCA is a very small molecule of about 150 Da (Michelakis *et al.*, 2008). DCA is cell permeable and targets cancer cells specifically with little or no effect on normal cells (Heshe, 2011). The absorption of DCA in the gastrointestinal tract has been found to be good and excretion of total DCA has been shown to be less than 1% (Stacpoole *et al.*, 1998).

Mechanism of action

DCA (figure 1.4) is a small molecule that has been used for decades for the treatment of lactic acidosis (Stacpoole *et al.*, 2008). It is known that cancer cells prefer to follow the glycolysis pathway as oppose to the OXPHOS pathway for glucose metabolism (Warburg, 1956). Pyruvate dehydrogenase (PDH) is a glycolytic enzyme that is responsible for the conversion of pyruvate to acetyl-CoA, which enters the tricarboxylic acid (TCA) cycle to generate ATP, thus promoting OXPHOS. But in cancer cells, the enzymatic activity of PDH is inhibited by an enzyme called pyruvate dehydrogenase (PDK) by a process called phosphorylation therefore prevents the entry of pyruvate into the TCA cycle which in turn results in less OXPHOS and more lactate production (Zhao *et al.*, 2011; Kato *et al.*, 2007). The preclinical trials on DCA have shown its effectiveness in a variety of cancer cells via induction of apoptosis (Bonnet *et al.*, 2007; Wong *et al.*, 2008). Treatment of DCA alone is still limited in ongoing trials but more effectiveness has been observed in combination therapy (Ishiguro *et al.*, 2012). The selective killing mechanism of DCA involves ROS production,

loss of mitochondrial membrane potential and apoptotic death (Ayyanathan *et al.*, 2012). Targeting PDK can result in a balance between OXPHOS and glycolysis. This results in the production of ROS that have been shown to be toxic to cancer cells. DCA has showed good activity against lung cancer cell line (A549) which resulted in increased ROS, preventing tumor growth and promoting apoptosis. These findings suggest that DCA would have no effect on normal non-cancerous cells (Bonnet *et al.*, 2007).

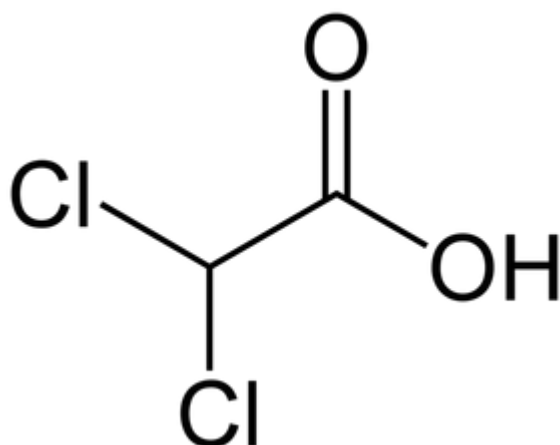


Figure 1.4: Chemical structure of Dichloroacetate (Michelakis *et al.*, 2008)

Methyl pyruvate (MP)

In normal cells, the OXPHOS pathway in the mitochondria generates 36 ATP molecules per glucose molecule broken down. However, cancer cells favour glycolysis which only generates 2 ATP molecules. MP can be used as a strategy to target this unique metabolism of cancer cells.

Methyl pyruvate is a derivative of pyruvate and this drug was used in this study to bypass the glycolytic pathway. Methyl pyruvate (MP) is a lipophilic agent in nature making it highly permeable to cells. MP is a favourable substrate than pyruvate as it is more stable (Lembert *et al.*, 2001; Düfer *et al.*, 2002). Since cancer cells prefer the glycolysis pathway, providing the end-product of this pathway might result in a circumvention of this pathway and thus lead to cell death. A recent study on A549 and MCF7 cells showed that treatment with

exogenous methyl pyruvate led to cell death (Monchusi and Ntwasa, 2017). Treatment with methyl pyruvate might boost OXPHOS and thus increases apoptosis by mechanisms such as production of ROS in the mitochondria (Lembert *et al.*, 2001; Düfer *et al.*, 2002).

1.12 Justification of study

Generation of ATP through the oxidative phosphorylation in the mitochondria is an efficient and preferred metabolic process, which produces far more ATP molecules (36 ATP molecules) from a given amount of glucose compared to glycolysis. In normal non-proliferating cells, OXPHOS is the preferred pathway for energy production and to a lesser extent glycolysis is used as another pathway which provides energy for cells. Upon infection however, cells like dendritic cells and macrophages tend to reprogram their metabolism in the same manner as the cancer cells. Cancer cells and proliferating cells show a deregulated metabolic profile by displaying an increased dependence on glycolysis for energy production and reduced levels of oxidative phosphorylation OXPHOS (Warburg effect). It is hypothesized that upon infection of cancer cells, a further metabolic reprogramming is expected. The two drugs (exogenous MP and endogenous DCA) to be used in this project have different mechanisms of action, but they both boost the mitochondrial OXPHOS. Theoretically it is expected that the application of the two drugs will reprogram the metabolism in such a way that cells are redirected to increased use of OXPHOS as an energy pathway and to a lesser extent, glycolysis (figure 1.5).

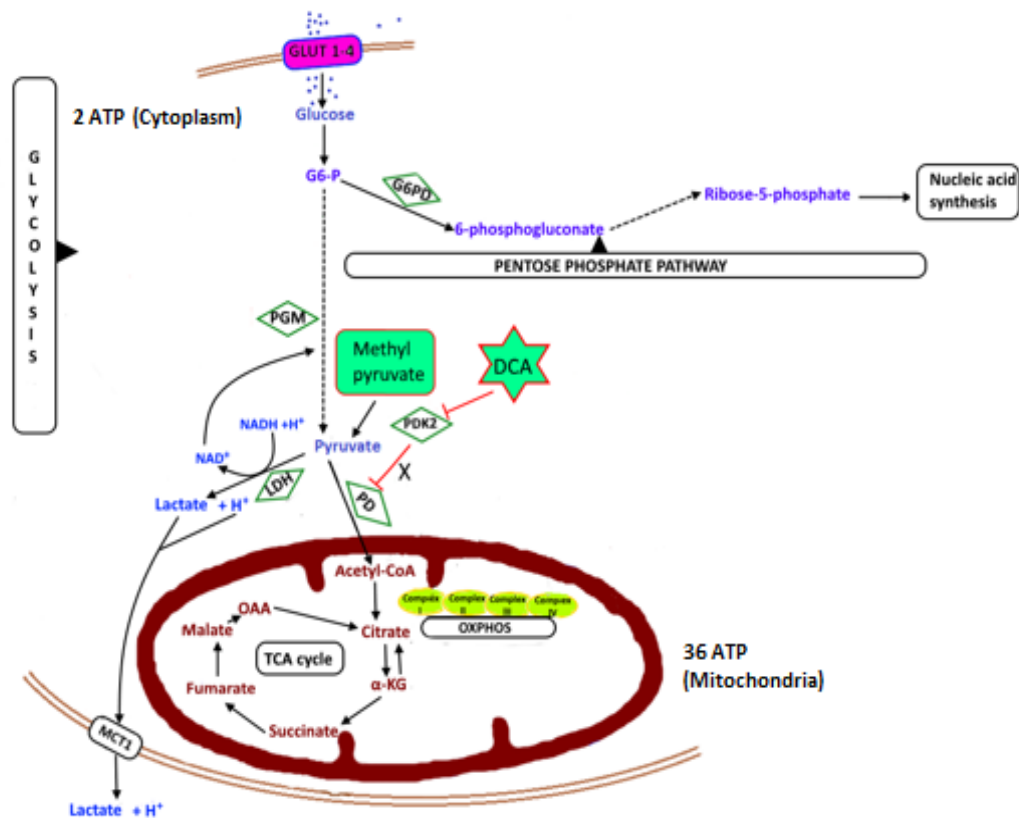


Figure 1.5: A simplified diagrammatic representation of the metabolic pathways (Glycolysis and OXPHOS): an illustration of how the energy metabolism shifts from glycolysis to OXPHOS when cells are treated with the two drugs (MP and DCA). Pyruvate entry into mitochondria is promoted, therefore an increase in OXPHOS is expected.

1.13 Aim

The aim of this study was to evaluate the molecular basis of metabolic reprogramming with a focus on the impact of drugs targeting mitochondrial function.

1.14 Objectives

- (i) To determine the expression of TLR4 in THP-1 cells before and after treatment with LPS using RT-PCR.
- (ii) To check the effect of various treatments on the cell cycle and cell viability using flow cytometry

(iii) To assay metabolic reprogramming by measuring the rate of glycolysis and OXPHOS in THP-1 cells before and after treatment with drugs.

CHAPTER 2: MATERIALS AND METHODS

2.1 Materials

Materials used in this study are listed under the appendix section. Appendix A has a list of chemicals and reagents, supplier and catalogue number. Appendix B consists of a list of laboratory equipment, supplier and model number. Appendix C, kits used, supplier and catalogue numbers. Lastly, Appendix D consists of a list of buffers and their composition.

2.2 Methods

This section describes methods (Figure 2.1) used in this study, to obtain the results that will be discussed in subsequent chapters. A brief introduction of the principle behind each technique is discussed, followed by the protocol of the technique.

2.2.1 An overview of the methods

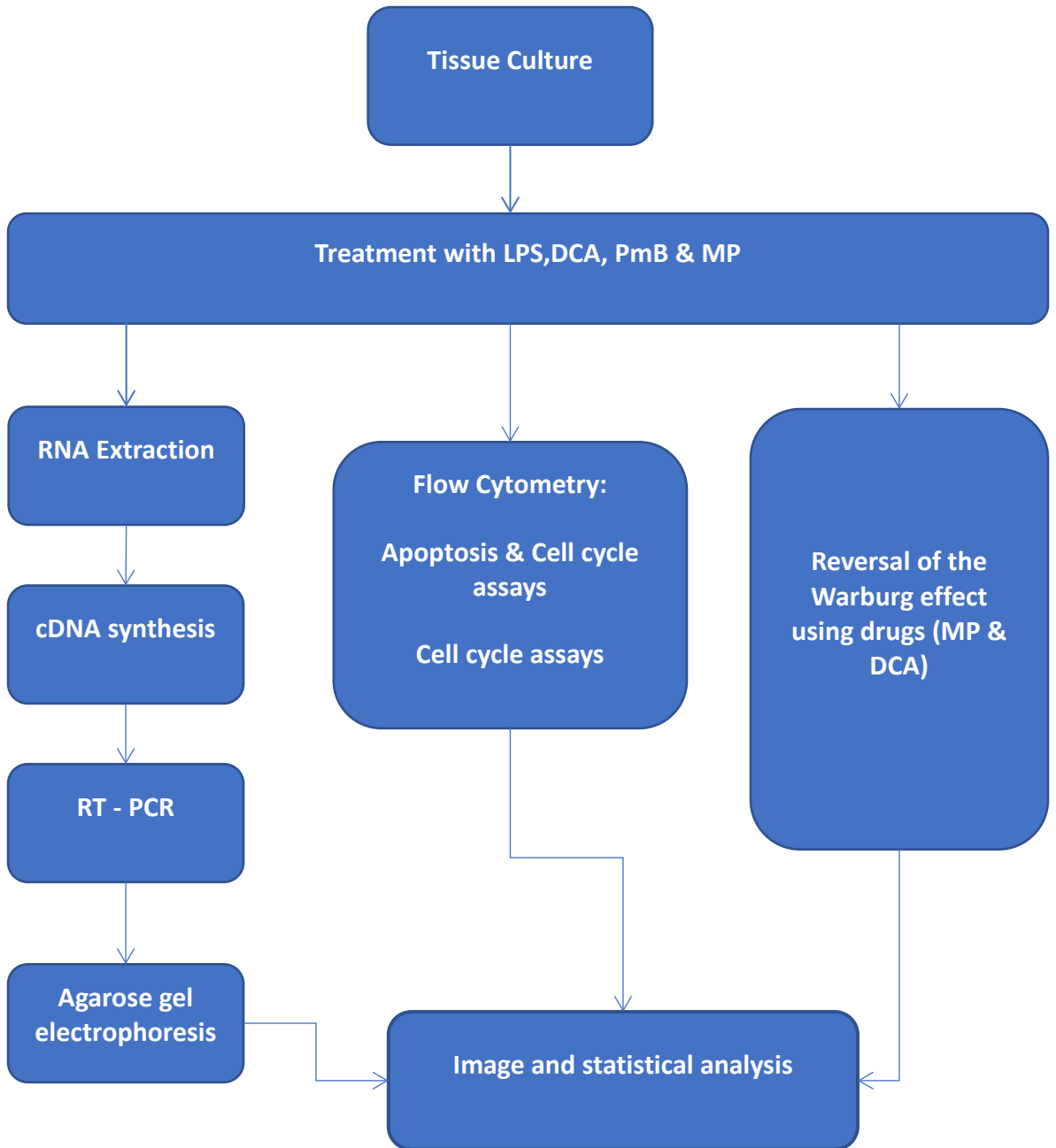


Figure 2.1 Flowchart diagram showing methods used in study. THP-1 cells were treated with LPS, DCA, PmB and MP. Following treatments, RNA extraction was performed, this was followed by flow cytometry assays and lastly Glycolysis and OXPHOS assays were performed.

THP1 cells were cultured under appropriate conditions and treated with several drugs (5 ng/ml LPS (from *Escherichia coli*), 10 mM DCA, 10µg/ml PmB and 0.08% MP) at varying time periods. First, total RNA was extracted from cells and

RT PCR performed to observe expression of TLR4. Second, Flow cytometry was performed involving cell cycle and apoptosis detection assays. Lastly, Glycolysis and OXPHOS assays were conducted to determine the effect of the drugs on cancer metabolism. These assays (apoptosis, cell cycle, glycolysis and OXPHOS) were performed in triplicates.

2.2.2 Cell line

THP-1 cells are derived from the peripheral blood of a 1-year old child with acute monocytic leukaemia. They have fc and C3b receptors and lack surface and cytoplasmic immunoglobins. These cells show increased CO₂ production on phagocytosis and can be differentiated into macrophages-like cells using compounds such as PMA.

2.2.3 Cell culturing routine and treatment

THP-1 cells were grown in RPMI growth medium supplemented with 10% FBS (fetal bovine serum) and 1% antibiotic (penicillin/streptomycin). These cells were routinely maintained in a humidified atmosphere at 37 °C in a 5% CO₂ incubator. THP-1 cells are a non-adherent cell line and have a doubling time of approximately 36-48 hours. These cells were sub-cultured every third day of the week by centrifuging cells with old medium 1500 rpm for 5 minutes. Following centrifugation, the pellet was resuspended in 1 ml of fresh medium. This was then transferred into 9 ml of fresh medium and incubated at 37°C in a 5% CO₂ incubator. The cultures were regularly examined using light microscopy (200x) for morphological signs of cellular damage.

2.2.4 Cell counting and viability determination

Cell counts are important as it helps to monitor growth rates. The cells were counted and the viability determined using the trypan blue exclusion test. Haematocytometer was used to estimate cell number using a thick glass with 2 counting chambers (1 on each side). Each of the counting chambers contains mirrored surface with 3 x 3 grids of 9 counting squares. Each of the 9 counting squares holds a volume of about 10 µl. About 10 µl of the cell suspension was transferred to 1 side of the chamber. The cell suspension was allowed to fill the entire counting chamber and placed under the microscope to view and count cells. All unstained cells in the central square of the grid were counted. The volume of

the grid is 10^4 ml therefore the number of cells per ml could be determined. The cells were counted and the viability determined using the trypan blue exclusion test. This formula was then used to estimate the number of cells/ml:

Number of cells/ml = Number of cells in central grid x 10^4 x dilution factor

Cells were treated with 5 ng/ml of LPS, 0.08% MP, 10 mM DCA and 10 μ g/ml PmB in time-dependant analyses. Time periods included 6,12,18 and 24 hours. Following treatment, cells were rinsed with about 1 ml PBS. One millilitre of trypsin-EDTA or citric saline buffer was added and incubated at 37 °C (for about 5-10 minutes, regularly checked the cell progression of cell dissociation). Following detachment of cells from the flask, trypsin activity was stopped by adding 1 ml of fresh culture medium. This mixture was centrifuged at 1500 rpm for 5 minutes, and supernatant discarded.

2.2.5 Cell cryopreservation and recovery

At regular intervals cells were removed from the cultures and stored frozen at -70°C. The cells were allowed to grow to the late log phase. A volume containing approximately 2×10^5 cells was removed from the flasks and the cells pelleted by centrifuging at 1500 rpm for 5 minutes at 20°C. The medium was discarded and the cells resuspended in 1 ml of freezing mixture. A volume of freezing mixture consisting of 10% DMSO and 90% FBS was added. The cell suspension was then transferred into sterile cryotubes and frozen slowly, wrapped in paper towel at -20°C overnight and then stored at -70°C until required. The cells were recovered from frozen storage by rapidly thawing in a water bath at 37°C. 9 ml of warm culture medium was added slowly to the cell solution to reduce osmotic shock. Centrifugation (1500 rpm for 5 min at 20°C) was used to remove the freezing solution, and the cells were resuspended in 9 ml of fresh culture medium. Cells were then placed in a small sterile tissue culture flask and maintained as previously described.

2.2.6 RNA extraction using TRIzol method

RNA extraction is a basic method that is used in molecular biology to extract biological material from the cell. Once extracted from the cell, RNA has shown to

have a very short life and is unstable. Therefore, it is important to extract RNA of good quality and to also avoid keeping RNA samples for a long period of time.

The medium containing cells (treated and untreated) was centrifuged at 3000 rpm for 3 minutes to obtain pellet. Cells were washed twice with 1X PBS. Attached cells (following treatment) were detached using trypsin, centrifuged at 1500 rpm for 5 minutes. Into each cell pellet, 500 μ l of TRIzol was added to each pellet and vortexed for 10 seconds for cell lysis and then kept on ice for 5 minutes. 250 μ l of chloroform was added and left to stand at room temperature for about 10 minutes. The tubes were centrifuged at 12 000 rpm for 15 minutes at 4°C for phase separation. The aqueous phase was removed and placed into newly labelled tubes. 250 μ l of Isopropanol was added into each tube and allowed to stand for 5 minutes at room temperature. The tubes were centrifuged at 12 000 rpm for 10 minutes at 4-8°C and supernatant discarded. 150 μ l of ice cold 70 % ethanol was then added to the pellet and centrifuged for 5 minutes at 12 000 rpm at 4°C to wash the RNA pellet thoroughly. The supernatant was discarded and pellet allowed to air dry for 7- 10 minutes. The tubes were then placed open on the heating block for 4 minutes to allow further evaporation of ethanol at 50°C. To dissolve the RNA pellet, 50 μ l of nuclease free water was added. The tubes were immediately placed on ice and the concentration and quality of RNA determined using a Nanodrop.

2.2.7 Complementary DNA synthesis (Reverse Transcription)

To perform RT-PCR, the obtained RNA template must first be converted into a complementary DNA (cDNA). In this study, this was done from 1 μ g of total RNA using the ProtoScript cDNA synthesis kit (NEB) according to the manufacturer's instructions. Table 2.1 show volumes of the different reagents used to make up the mixture for cDNA synthesis. Cycling conditions used were those indicated by the manufacturer.

Table 2.1: cDNA synthesis reagents.

| Components | Volume (µl) |
|-----------------------|--------------------|
| Oligo Dt | 1 |
| d NTP mix | 1 |
| Total RNA | 3 |
| Nuclease Free water | 9 |
| Sub-Total | 14 |
| 5X SSIV buffer | 4 |
| DTT | 1 |
| Reverse Transcriptase | 1 |
| Total volume | 20 |

2.2.8 Polymerase Chain Reaction (PCR)

Polymerase chain reaction (PCR) is a technique used for DNA replication, that allows target DNA sequences to be amplified into millions of copies. This technique involves the primer mediated enzymatic amplification of DNA. Primer sequences were identified and synthesized by Inqaba biotech. The cDNA obtained through reverse transcription was used as a template using sequence specific primers for the TLR 4 gene. The PCR was performed using Taq 2X master mix. Reagents were mixed appropriate (table 2.3) using gene specific primers (table 2.4). The master mix already contains deoxyribonucleotides, PCR buffer, MgCl₂ and Taq Polymerase. PCR conditions are shown in table 2.2.

Table 2.2: PCR cycling conditions and time spent per cycle.

| STEP | TEMPERATURE | TIME |
|----------------------|-------------------------|-----------------------------------|
| Initial Denaturation | 95°C | 30 secs |
| PCR cycles (30) | 95°C 45-68°C 68°C | 15-30 secs 15-60 secs 1 min |
| Final Extension | 68°C | 5 mins |
| Hold | 4°C | - |

Table 2.3: PCR 50 µl reaction mixture

| Component | 50 µl Reaction |
|-----------------------|-----------------------|
| 100 µM Forward Primer | 0.5 µl |
| 100 µM Reverse Primer | 0.5 µl |
| Template DNA | 3 µl |
| Taq 2X Master Mix | 25 µl |
| Nuclease free water | 21 µl |

Table 2.4: Primers used for TLR 4 mRNA expression.

| TLR | Forward primer | Reverse primer |
|------------|---------------------------------|-----------------------------------|
| GAPD H | 5' GAAGGTGAAGGTCGGAGTC 3' | 5' GAAGATGGTGATGGGATTT C 3' |
| TLR 4 | 5'CCAGTGAGGATGATGCCAGA AT 3' | 5'GCCATGGCTGGGATCAGA GT 3' |

2.2.9 Agarose gel electrophoresis

The principle of agarose gel electrophoresis involves separation of nucleic acids according to their size using an electric field. Whereby negatively charged molecules migrate towards the anode (positive) side. This migration is determined by molecular weight, small molecules migrate faster than large molecules. During this technique the DNA fragments can be visualized by staining the gel with ethidium bromide, which is a dye that intercalates between bases of DNA and illuminates the gel under UV light source. About 1g of agarose powder (1% agarose gel) was dissolved in 50ml of 1x TAE buffer and heated until the agarose was completely dissolved in TAE. This mixture was further cooled to about 50°C and 3 µl (0.8 mg/ml) of ethidium bromide added. Mixture was poured onto a

casting tray, placed a comb and allowed the gel to solidify. Once solidified, the comb was carefully removed and gel placed inside a tank containing 1x TAE buffer. The samples were loaded into individual wells, with the first well used for a DNA marker, connected the tank to a power supply and ran the samples at 90 volts for about 45 minutes. The gel was then visualized under the Bio-Rad Gel doc system.

2.2.10 Flow cytometry

Flow cytometry is a technique that measures and analyses physical properties of cells as they flow in a fluid medium through a laser beam. Measurements include size, granularity, and fluorescence (Brown and Wittwer, 2000). In this study, flow cytometry was used to assess apoptosis, necrosis and cell cycle analyses following treatment with LPS, PmB, DCA and MP. For all drug treatments, cells were seeded at a density of 2×10^5 cells/ml in 6-well plates. Drugs were added in a time-dependant manner at 6,12,18 and 24 hours respectively and cells were incubated under culturing conditions mentioned above.

Phosphatidyl serine (PS) is a cell membrane phospholipid that plays an important role in cell cycle signalling. During the early phases of apoptosis, PS which is embedded within the plasma membrane of live cells becomes translocated to the external surface of the cell membrane. The externalisation of PS is used as a marker of early apoptosis. Annexin V is a calcium ion-dependent protein that has a high binding affinity for PS. Annexin V coupled to the green fluorescent dye, FITC can be used to assess the level of apoptosis using a flow cytometer (Koopman *et al.*, 1994). During necrosis cell death, the plasma membrane integrity becomes compromised which results in the exposure of DNA. The exposure of DNA is taken advantage of by the DNA-binding dye, propidium iodide, as a marker of necrosis.

Cell cycle assay

Cell cycle analysis is achieved by using fluorescent nucleic acid dyes such as PI (Propidium iodide). PI make use of the fact that DNA contents change as the cell progresses from the G1, S and G2 phases of the cell cycle. Cells that are in the S-phase of the cell cycle have more DNA than those in the G1. While G2 cells have

approximately doubled the amount of DNA found in G1 cells. For cell cycle analysis, cellular DNA content is measured using the DNA-binding dye, PI. PI intercalates into the helical structure of DNA. The amount of fluorescence yield of PI is directly proportional to the amount of DNA present within the cell (Brown and Wittwer, 2000). This makes it easy to detect cells that have undergone growth arrest at any phase of the cell cycle.

Cells were harvested by centrifugation at 1500 rpm for 5 minutes. Pellet formed was washed twice with PBS (to remove the medium). The cells were then fixed. Fixation of the cells was done using 70% (v/v) ethanol. Ethanol is a dehydrating fixative agent which also permeabilizes the cells to allow for the binding of PI to DNA. The cells were treated and harvested with about 1 ml trypsin. The cells were pelleted by centrifugation at 1500 rpm for 10 minutes and cell pellet was carefully resuspended in 1 ml of PBS in a 1.5 ml eppendorf tube. The mixture was centrifuged for 5 minutes at 5000 rpm and the pellet was resuspended in 300 μ l of PBS. Seventy microliters of 100% ethanol (pre-chilled at -20°C) was added to each sample and mixed by inverting the tube 5 times. The cell suspension was centrifuged at 5000 rpm for 5 minutes, after which the supernatant was removed. The pellet was then washed twice with 1 ml of PBS, followed by centrifuging at 1500 rpm for 7 minutes. The PBS supernatant was discarded, and pellet resuspended in 300 μ l of PI containing RNase and vortexed for 30 seconds. The cell suspension was then incubated in the dark for 30 min, after which cell cycle analysis were done at 488 nm using the BD Accuri C6 flow cytometer.

Apoptosis assay

To ascertain whether the cell death observed is by apoptosis and not necrosis, cell viability assays were performed using flow cytometry. Healthy cells have an intact plasma membrane while apoptotic cells display loss of plasma membrane. In early apoptotic cells, the membrane phospholipid phosphatidyl serine (PS) is translocated from the inner to the outer leaflet of the plasma membrane, thereby exposing PS to the external cellular environment. Annexin V is a 35-36 kDa Ca^{2+} dependent phospholipid-binding protein that has a high affinity for PS and binds to the exposed PS.

Staining with Annexin V is used in conjugation with dyes such as propidium iodide (PI) to allow identification of early apoptotic cells (PI negative, FITC Annexin V positive). Viable cells with intact membrane cannot bind PI while damaged cells can. Viable cells are both Annexin V and PI negative. Cells that are in early apoptosis are considered Annexin V positive and PI negative, and cells that are in late apoptosis are both Annexin V and PI positive.

Following treatments with apoptosis-inducing agents/drugs (MP and DCA) for 24 hours, the culture media was collected from the 6 well plates and centrifuged at 1500 rpm for 5 minutes to collect pellets. Cell pellets were then washed in 600 μ l cold PBS and centrifuged at 1800 rpm for 5 minutes. Supernatant was discarded and cells resuspended in 1x annexin-binding buffer. About 5 μ l of Alexa Fluor 488 annexin V and 1 μ l of 100 μ g/ml PI solution were added to each 100 μ l of cell suspension and incubated at room temperature for 30 minutes. Following the incubation period, 400 μ l of 1X annexin-binding buffer was added, this was mixed gently and kept on ice. Samples were immediately analysed using the BD Accuri flow cytometer by measuring fluorescence emission at 530nm.

2.2.11 Glycolysis and OXPPOS assays

Oxygen consumption and Glycolysis measurements were performed following the treatments with drugs (LPS, PmB, DCA and MP) in order to measure the degree of the reversal of the Warburg effect displayed by the THP-1 cancer cells. The Cayman's oxygen consumption /Glycolysis dual assay kit is a multi-meter approach used to measure cellular oxygen consumption and glycolysis in living cells. MitoXpress Xtra is used to measure oxygen concentration rate while extracellular lactate is quantified as an indication of glycolysis. The kit was used for measuring the effect of drugs that modulates the cell metabolism.

OXPPOS assay

THP-1 cells were treated at various concentrations of (LPS, MP, DCA and PmB) at concentrations mentioned above. 100 μ l of cells were seeded at a density of 65000 cells/well in a black, clear bottom 96-well tissue culture treated plate. The cells were incubated at 37°C at 5% CO₂ concentration for 24 hours. After 24

hours of incubation, 50µl of cells (65 000 cells/well) was added to each well to obtain a total volume of 150 µl per well. 10 µl of each drug (LPS, MP, DCA and PmB) was transferred to each well and 10µl of MitoXpress Xtra solution added. A blank (containing medium only) served as a control for this assay. The wells were overlaid with 100µl of pre-warmed HS Mineral oil and plate was read kinetically for ≥ 120 minutes on a plate reader.

Glycolysis assay

This assay was performed with the same samples for oxygen consumption measurements performed above but on a new clear 96-well tissue culture treated plate. Ninety microliters of the assay buffer was added to each well and 10 µl of mixture containing samples transferred to the well. 100 µl of reaction solution was then added to all wells and plate incubated on an orbit shaker for 30 minutes at room temperature. The absorbance was read at 490nm with a plate reader.

2.3 Image and statistical analysis

Image analysis of captured agarose gels were quantified using MyImage analysis software tool. Optical densities were exported to Microsoft Excel for normalisation. The results of each series of experiments (performed in triplicates) were exported to Microsoft excel and the mean values \pm standard deviation of the mean (SD) calculated. Levels of the statistical significance were also calculated using the paired student t-test when comparing two groups. P-values of ≤ 0.05 were considered significant.

CHAPTER 3: RESULTS

3.1 Overview

In this study, the expression of TLR4 in LPS- induced THP1 cells was investigated and it was observed that 5 ng/ml LPS was optimal in inducing the expression of TLR4. An overexpression of TLR4 was also observed in untreated THP-1 cells which is suggesting constitutive expression. Cell cycle analysis showed that treatment with DCA did not have any impact on the cell progression of THP-1 cells. However, cell cycle progression was observed in THP-1 cells treated with exogenous MP. Further analysis of cell death showed that MP and DCA treated cells resulted to very minimal apoptotic cell death and decrease in necrosis compared to untreated and LPS-treated cells. This suggests that the 2 drugs cause cell death via apoptosis. In contrary, LPS-treated THP-1 cells showed an increase in necrotic cells compared to untreated and other treatments. Also, it was observed that treatment with MP and DCA boosted OXPHOS pathway, while exogenous MP reduced glycolysis suggesting that this drug indeed reversed metabolic reprogramming in THP-1 cells. However, endogenous DCA did not show any reduction in glycolysis. Furthermore, LPS treated cells did not show an increase in glycolysis, meaning the expected “double” Warburg effect was not observed.

3.2 Expression of TLR 4 in THP-1 cells using RT-PCR

To ascertain the optimal concentration of LPS to induce expression of TLR-4 in THP-1 cells, RT-PCR was performed. Cells were seeded and then treated at 5 ng/ml, 10 ng/ml and 20 ng/ml LPS concentrations for 24 hours and total RNA was extracted and RT-PCR was performed. The differential expression of TLR 4 was observed at various concentrations of LPS (Figure 3.1). THP-1 cells serve as both innate immune and cancer cell-line. LPS is a component that is found on the cell wall of gram negative bacteria and it was used in this study to mimic the bacterial infection in cancer.

When THP-1 cells were treated with 5 ng/ml of LPS, TLR 4 was observed to be the most over-expressed compared to at 10 ng/ml and 20 ng/ml. These results show that 5 ng/ml of LPS is optimal for the induction of TLR 4 expression. This concentration was used for downstream experiments. These results also show that indeed LPS is an agonist for TLR 4.

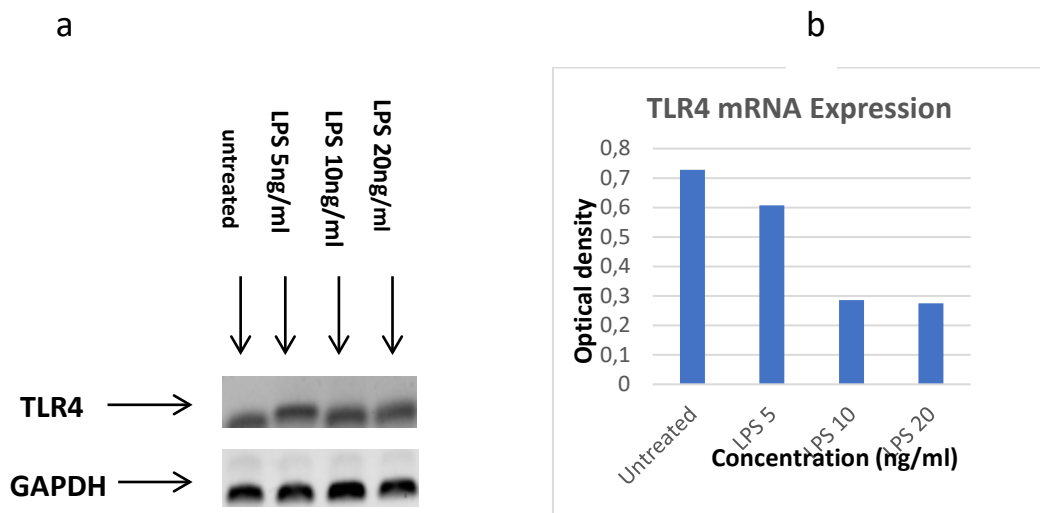


Figure 3.1: TLR 4 expression in untreated and LPS-stimulated THP-1 cells a) Agarose gel electrophoresis showing mRNA expression levels in LPS (5, 10, 20 ng/ml) induced THP-1 cells. (b) Densitometry results of mRNA levels at various treatment concentrations.

3.3 Cell cycle analysis of THP-1 human monocytic cells following various treatments in a time-dependant analyses.

To determine the cell cycle changes following various treatments, flow cytometry was performed. THP-1 cells were treated with 0.08% MP and 10mM DCA and combination with 5 ng/ml LPS and 10 µg/ml PmB. Following treatments, cells were harvested at different intervals of (6,12,18 and 24 hours). Treatment with MP seems to promote cells cycle progression at G2/M phase after 24 hours of treatment at about 11.4%, which is about 3 times to that observed for DCA and other treatments. This cell cycle progression was only observed in MP-treated cells across all time-intervals. Experiments were done in triplicates. Figure 3.2

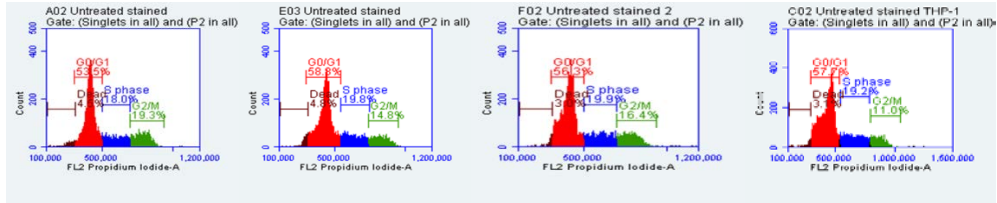
show time-dependant cell cycle phases at 6,12,18 and 24-hour intervals following treatments with 5ng/ml LPS, 10mM DCA, 10 µg/ml PmB, and 0.08% of MP.

6 hours

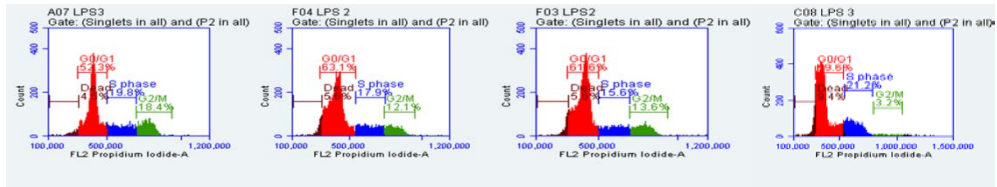
12 hours

18 hours

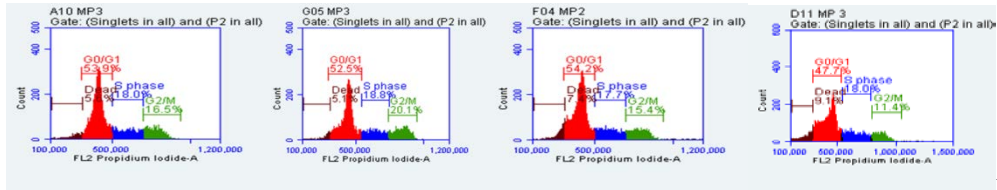
24 hours



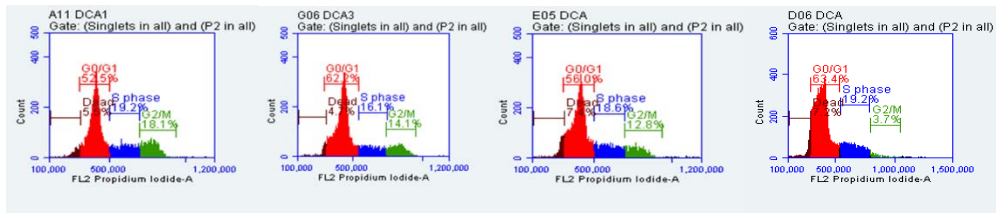
Untreated



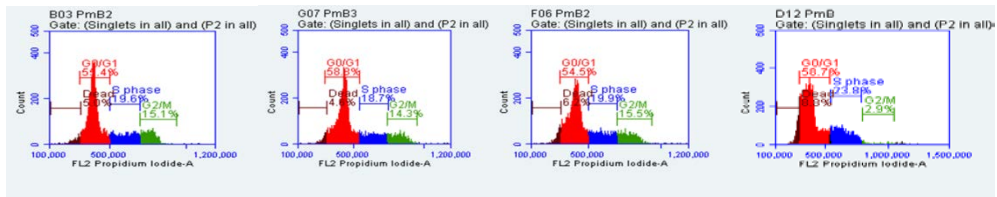
LPS



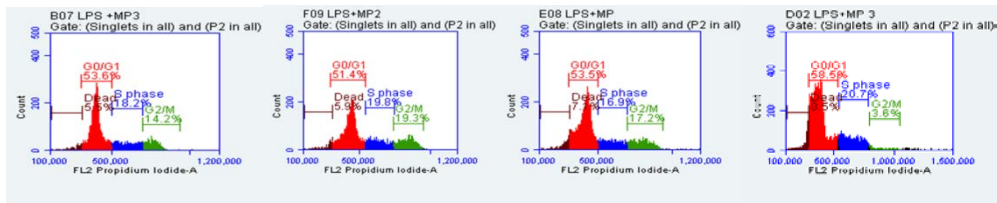
MP



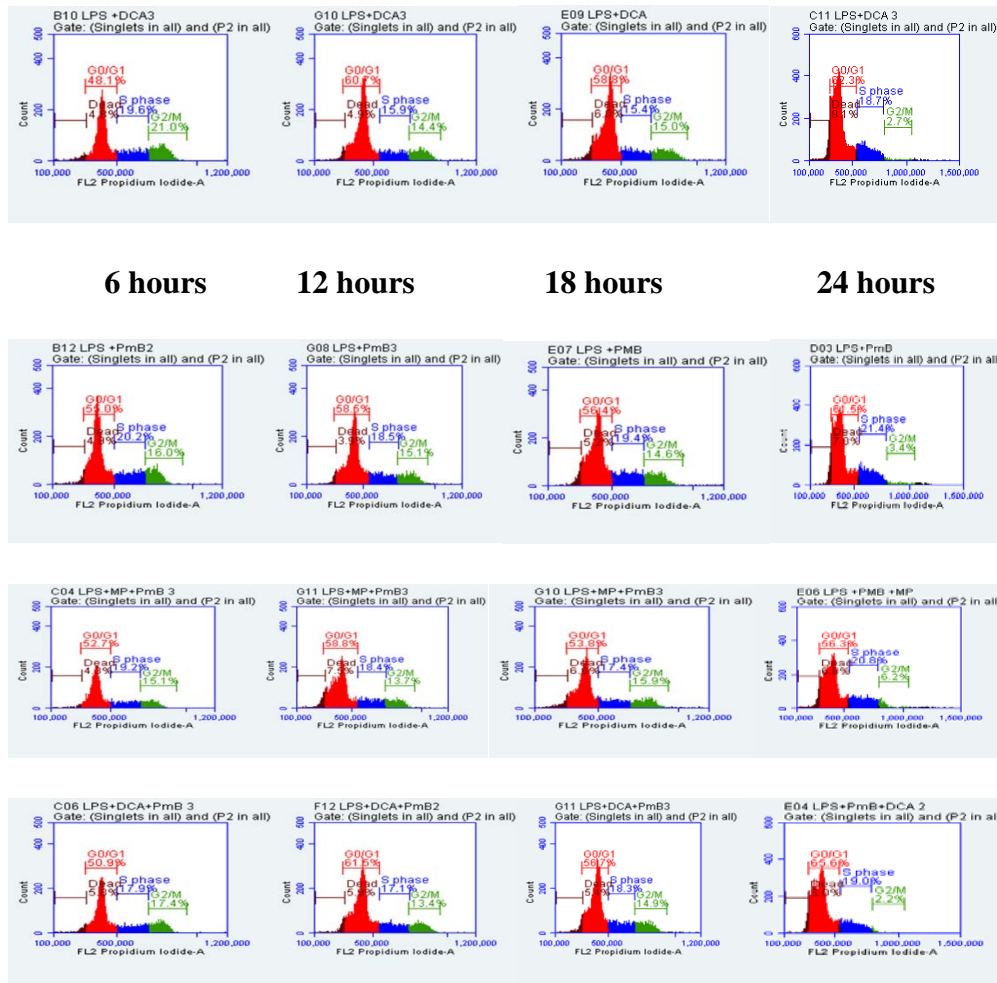
DCA



PMB



LPS+MP



LPS+DCA+PmB

Figure 3.2: The effects of various drugs treatments on the cell cycle progression in THP-1 cells at various time intervals (6, 12,18, and 24 hours). As shown, cells in the Sub-G0 phase (red) represent apoptotic and necrotic THP-1 cells. 5 ng/ml LPS (Lipopolysaccharides), 10 mM DCA (Dichloroacetate), 0.08 % MP (Methyl pyruvate), 10 µg/ml PmB (Polymyxin B). The cell cycle assay was performed using BD Acurri™ flow cytometer. The data represented here is a representative of three separate experiments.

At 6, 12,18 and 24 hours of treatment, LPS has no influence on the cell cycle, cells seem to stay at G0 with little progression to G2/M. Reversal of the Warburg effect with drugs also has no effect on cell cycle. At G0/G1, it does not matter what treatment is used on THP-1 cells, it does not change. S phase seems to be downregulated in most treatments. Across all treatments, there is a progressive decline of the S phase (cells undergoing DNA replication). Even in the presence

of drugs (MP and DCA), which are involved in the disruption of metabolic reprogramming, these drugs still do not influence the cell cycle of LPS. From all these observations, MP alone seems to be the only drug that has any influence in the cell cycle of THP-1 cells as oppose to DCA, MP does not reverse progression. This drug does not change the proliferative state of the cells. PmB (which neutralises LPS) also has no effect on the cell cycle even at 24 hours (Figure 3.6).

3.3.1 Distribution of cells in sub G0/G1 phase after treatment

From the cell cycle results, sub-G0 cells from Figure 3.2 indicate cell death, this cell cycle phase is easily distinguishable from other phases because cells in this phase are characterized by DNA that is less than $2n$. After 6, 12 and 18 hours of treatment (Figure 3.3,3.4 and 3.5 respectively), it was observed that all the treatments had no effect on the proliferative state of the cells. Exogenous MP and endogenous DCA show the highest death at sub-G0 with 7.4 and 7.5% respectively, following 18 hours of treatment. When cells were treated with a combination of LPS and DCA at 24 hours, 9.1% of cells were observed in the sub-G0 phase. Interestingly, after 24 hours of treatment with MP alone, 9.1% of cells were in the sub-G0 phase. These results are not surprising, because these drugs target the metabolism of cancer cells but they do not cause any DNA damage to the cells therefore, not many cells were observed in the sub G0/G1 phase.

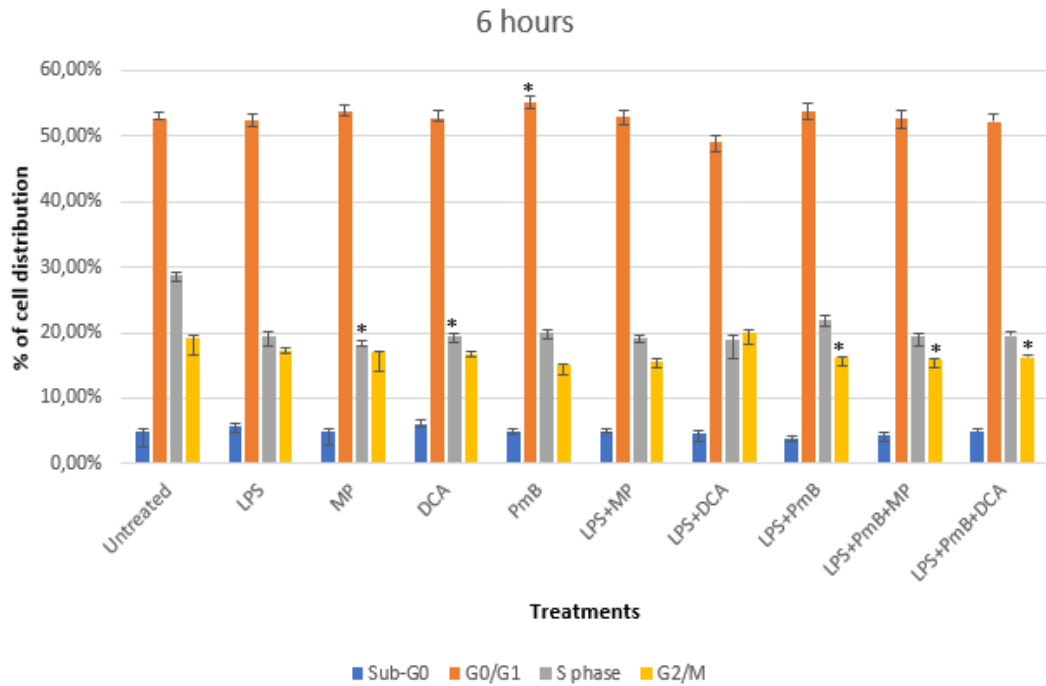


Figure 3.3: Cell cycle analysis in THP-1 human monocytic cells. Cells were treated with 10ng/ml of LPS, 0.08 MP, 10mM DCA and/or 10 μ g/ml PmB for 6 hours. Data is represented as mean \pm SD from 3 independent experiments (* indicates $p < 0.05$, ** indicates $p < 0.01$, *** indicates $p < 0.001$).

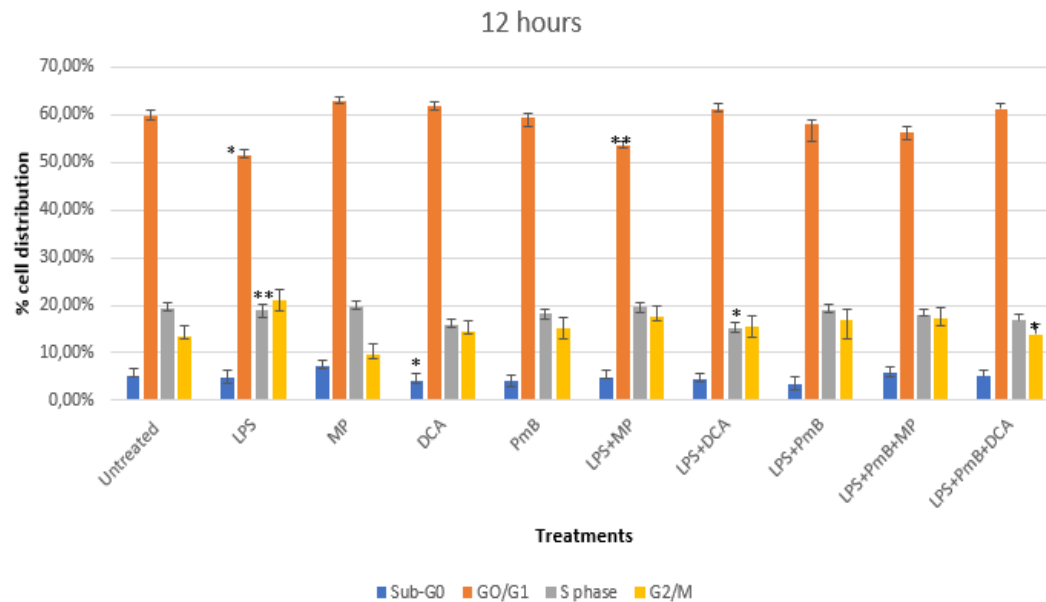


Figure 3.4: Cell cycle analysis in THP-1 human monocytic cells. Cells were treated with 10ng/ml of LPS, 0.08 MP, 10mM DCA and/or 10ng/ml PmB for 12 hours. Data is represented as mean \pm SD from 3 independent experiments (* indicates $p < 0.05$, ** indicates $p < 0.01$, *** indicates $p < 0.001$).

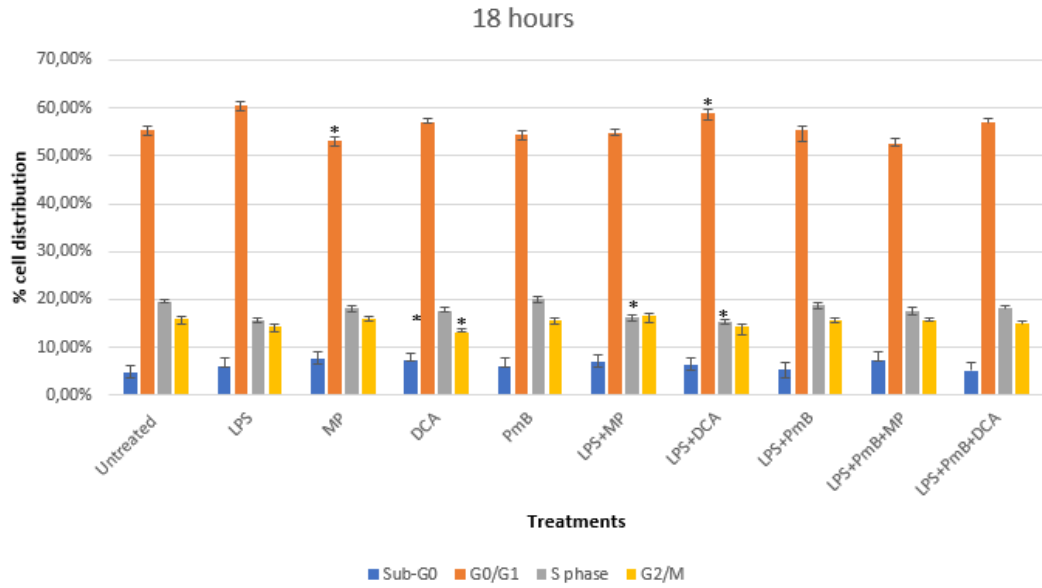


Figure 3.5: Cell cycle analysis in THP-1 human monocytic cells. Cells were treated with 10ng/ml of LPS, 0.08 MP, 10mM DCA and/or 10 μ g/ml PmB for 18 hours. Data is represented as mean \pm SD from 3 independent experiments (* indicates $p < 0.05$, ** indicates $p < 0.01$, *** indicates $p < 0.001$).

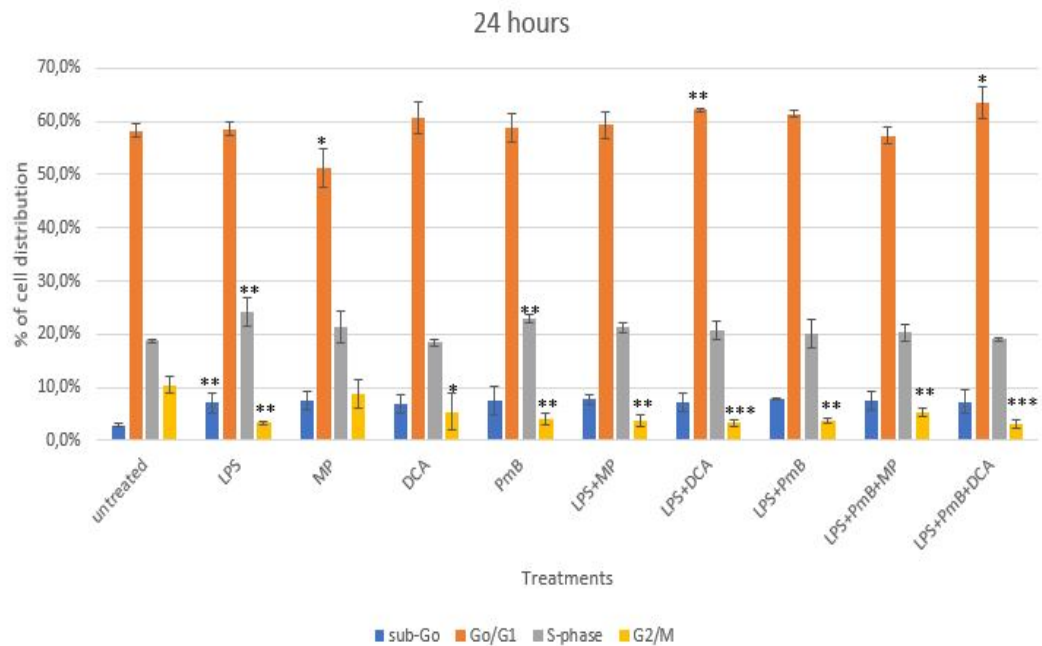
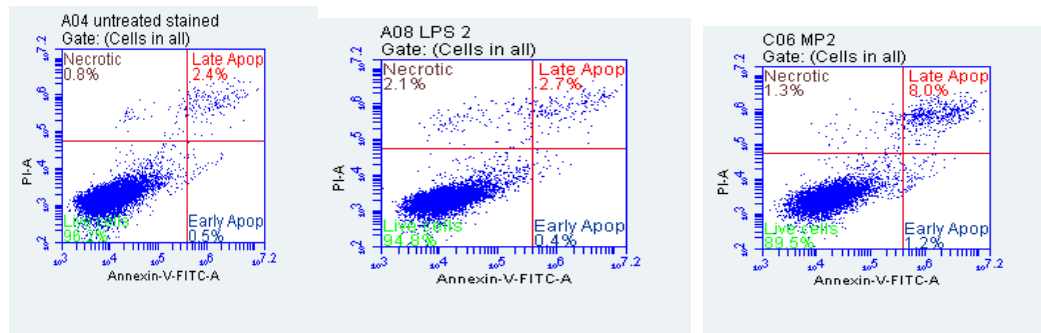


Figure 3.6: Cell cycle analysis in THP-1 human monocytic cells. Cells were treated with 10ng/ml of LPS, 0.08 MP, 10mM DCA and/or 10 μ g/ml PmB for 12 hours. Data is represented as mean \pm SD from 3 independent experiments (* indicates $p < 0.05$, ** indicates $p < 0.01$, *** indicates $p < 0.001$).

3.4 Apoptosis induction following various treatments.

To show whether the observed death was due to apoptosis or necrosis, flow cytometry assay was used. This was achieved by using Annexin V and PI staining which makes it possible to distinguish between cells that are undergoing apoptosis (early and late) and necrotic cells. In this study, cells were treated with the various drugs for 24 hours and the cell death observed was analysed to be either via apoptosis and necrosis.

The phosphatidyl serine (PS) of normal cells is located on the cytoplasmic surface of the cell membrane. But in apoptotic cells, PS becomes exposed to the external environment. Annexin V binds to this PS therefore one can distinguish between apoptotic and necrotic cells. PI is a nucleic acid binding dye. This dye does not stain live cells or apoptotic cells, but it only stains dead cells, and binds to the nucleic acid in the cell. Flow cytometer system is used to distinguish between these different populations. Results show percentages of apoptotic and necrotic cell death (Figure 3.7).



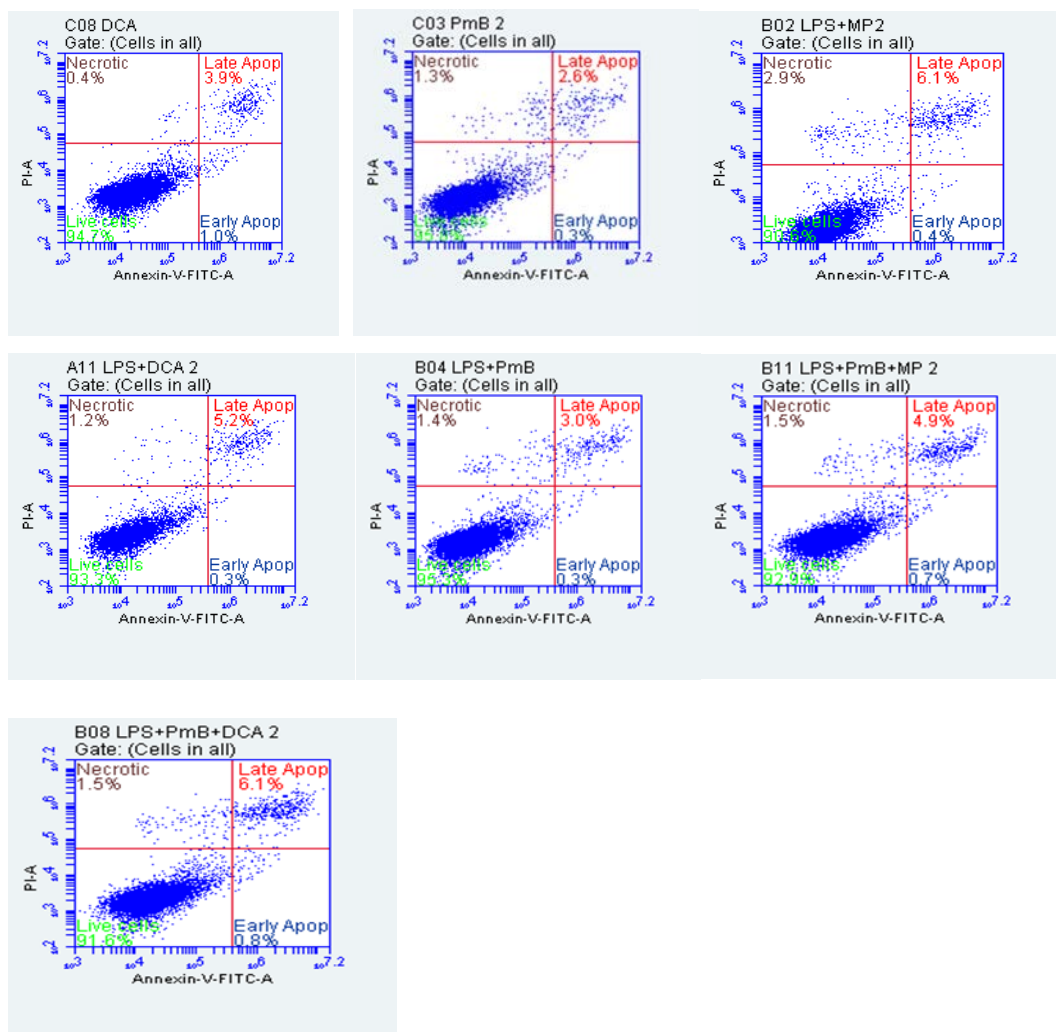


Figure 3.7: Effects of various treatments on inducing apoptosis in THP-1 cells following 24 hours of treatment. Each diagram represent a treatment. Annexin V/PI stained THP-1 cells following treatment with either 5 ng/ml LPS, 0.08% MP, 10mM DCA, 10 µg/ml PmB and combination of these treatments in comparison with untreated cells for 24 hours. Each of the quadrants represents populations of viable (lower left), early apoptotic (lower right), late apoptotic (upper right) and necrotic (upper left) cells.

Results show that induction of apoptosis using drugs such as MP and DCA THP-1 cells was fairly low (9.2 % and 4.9% respectively) compared to untreated cells (2.4%) (Figure 3.8). On the other hand, cell death by necrosis was only 1.3% and 0.4% for MP and DCA treated cells respectively. This suggests that cell death during treatment with DCA is mostly by apoptosis. However, it was observed from figure 3.8 that treatment of THP-1 cells with exogenous MP alone promotes

both apoptosis and necrosis. When cells were treated with LPS, cell death was due to necrosis and not apoptosis with about 2.1% necrotic cell death compared to 0.8% observed in untreated. This suggests that during infection, there is an increase in necrotic cell death. Necrosis in tumours have been observed to result to poor prognosis. Only (6.5% and 5.5%) increase in apoptosis was observed in THP-1 cells treated with LPS and MP or DCA respectively. Cells treated with LPS and PmB showed similar results to those observed in untreated THP-1 cells. This is not surprising as, PmB blocks the activity of LPS therefore results will resemble those of untreated cells (control).

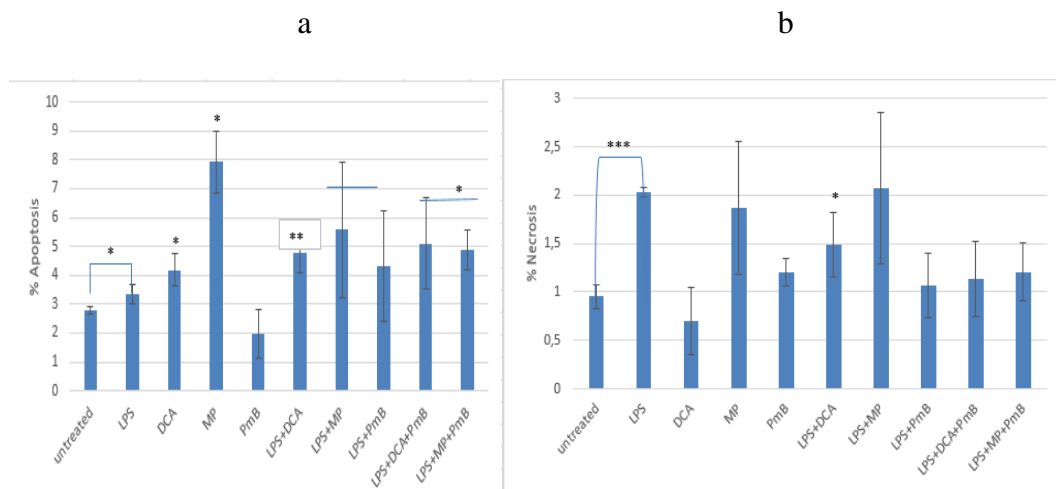


Figure 3.8: Statistical analysis of flow cytometry results-obtained a) apoptosis and b) necrosis (%) in THP-1 cells following 24 hours of treatment. T-test was used to generate the p-values which compared the difference between the untreated and treated scores. Data is represented as mean \pm SD from 3 independent experiments (* indicates $p < 0.05$, ** indicates $p < 0.01$, *** indicates $p < 0.001$).

3.5 Glycolysis and OXPHOS assays following treatment with drugs that reverse the Warburg effect.

The glycolysis and OXPHOS assays were performed to measure the effect of the drugs (MP and DCA) on the metabolism of THP-1 cells following 24 hours of treatments. Exogenous MP is known to reverse the metabolism of cancer cells by avoiding the glycolytic pathway and thus may shift the metabolism to OXPHOS. DCA on the other hand, acts endogenously by inhibiting an enzyme called PDK, which (in its active form) phosphorylates PDH and renders it inactive therefore

more pyruvate is converted into lactate as oppose to entering the TCA cycle and then OXPHOS. In this section, we measured the effect of drugs in the reversal of the Warburg effect. The following results were obtained by measuring each pathway independently following various treatments (Figure 3.9-3.10).

Cells treated with MP showed reduced levels of glycolysis as compared to the untreated cells (Figure 3.9) while showing an increase in OXPHOS pathway (Figure 3.10) suggesting a shift from glycolysis to OXPHOS. Interestingly, MP-treated cells have the highest rate of OXPHOS compared to the untreated and all the other treatments. Exogenous pyruvate boosts OXPHOS as it directly goes to the TCA, thereby interfering with the Warburg effect (Monchusi and Ntwasa, 2017). Furthermore, THP-1 cells treated with DCA showed more dependence on OXPHOS as compared to the untreated cells indicating that DCA was able to inhibit the enzyme PDK and thereby enabling some pyruvate to be converted into the TCA cycle. DCA -treated cells, in contrary to MP-treated THP-1 cells still showed some dependence on the glycolytic pathway. DCA inhibits PDK and enhances the conversion of pyruvate into the TCA cycle, however, this drug acts endogenously, suggesting some of the pyruvate can still be converted into lactate as proven by the increased levels of L-lactate concentration in DCA-treated THP-1 cells. Even in the presence of LPS which mimics infection, therefore aggravating the Warburg effect, MP still boosted OXPHOS compared to untreated cells. LPS treated cells showed more dependence on the glycolytic pathway and less dependence on OXPHOS. This was expected because it is known that upon infection, innate immune cells reprogram their metabolism in a manner that is similar to the one observed in cancer cells (Warburg effect), and THP-1 cells are both innate immune and cancer cells therefore they should display an increased Warburg effect. THP-1 cells treated with LPS+DCA showed similar results as those observed in DCA only treated cells, whereby cells show slightly more dependence on OXPHOS but also promotes the use of the glycolysis pathway still. PmB treatments did not show any significant changes when compared to the untreated cells. But PmB was only used to block the effect of LPS (a component found on the outer layer of gram negative bacteria) since PmB is an antibiotic therefore kills gram negative bacteria.

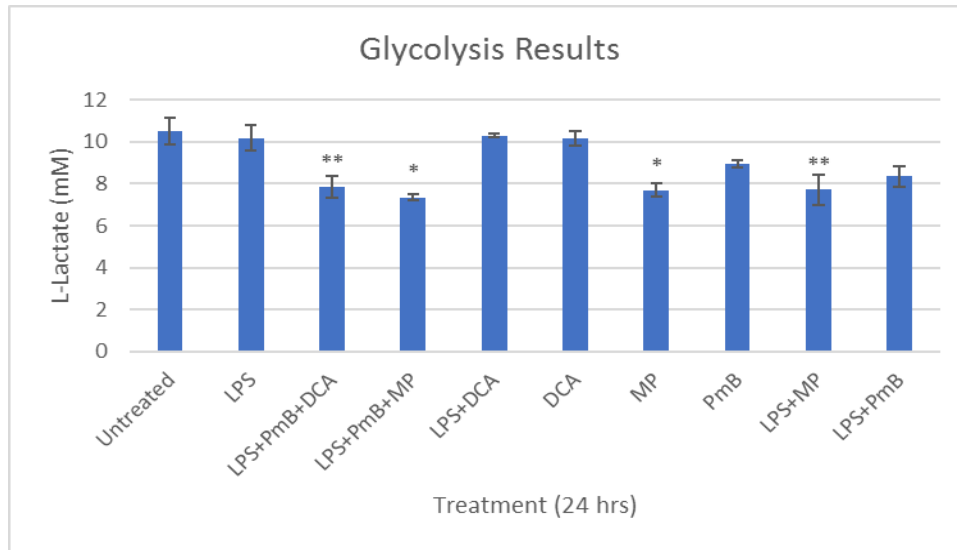


Figure 3.9 Glycolysis was analysed in THP-1 cells using the Cayman’s dual assay kit system which relies on measurement of lactate (indication of the glycolytic activity) in 96 well plates following various treatments for 24 hours. These values were exported from the plate reader and exported to excel for analysis. Data is represented as mean \pm SD from 3 independent experiments (* indicates $p < 0.05$, ** indicates $p < 0.01$, *** indicates $p < 0.001$).

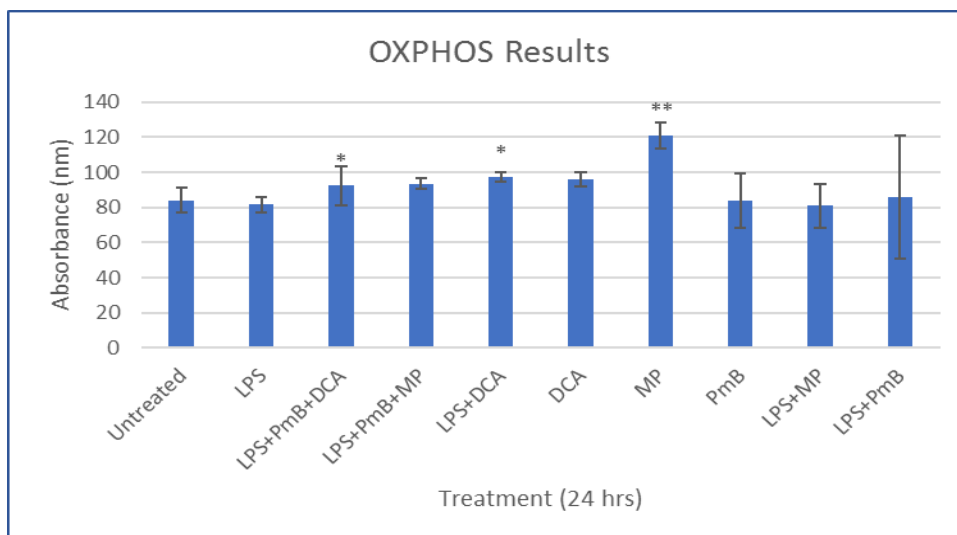


Figure 3.10: OXPHOS was analysed in THP-1 cells using the Cayman’s dual assay kit system which relies on measurement of quenched oxygen (indication of OXPHOS activity) in 96 well plates following various treatments for 24 hours. The values were exported from the plate reader and exported to excel for analysis. Data is represented as mean \pm SD from 3 independent experiments (* indicates $p < 0.05$, ** indicates $p < 0.01$, *** indicates $p < 0.001$).

CHAPTER 4: DISCUSSION

This study sought to investigate the molecular basis of metabolic reprogramming in innate immune cells. The role of exogenous MP in reversing the Warburg effect in cancer cells and the effect thereof was also observed. This study has shown that by bypassing the glycolytic pathway using drugs such as MP, you subsequently promote OXPHOS while suppressing glycolysis. Since cancer cells rely on the glycolytic pathway for energy generation (Warburg effect), drugs such as MP and DCA that disrupt the Warburg effect resulted in death by apoptosis (although very minimal). Surprisingly when endogenous DCA was used to treat cells, it did not result to decreased levels of glycolysis.

Flow cytometry analysis showed that the percentage of apoptotic THP-1 cells following treatment with MP and DCA was fairly low. Cancer cells avoid the OXPHOS pathway as it is detrimental to them. For example, the production of ROS which is a consequence of this pathway leads to toxicity.

Also, LPS-treated THP-1 cells show an increase in necrosis. Necrosis in tumours have been observed to indicate migration and even metastasis. This observation may indicate that infected cancer cells might be more aggressive.

4.1. TLR 4 is overexpressed in untreated THP-1 cells compared to the LPS-treated cells.

Innate immune response to stimuli such as LPS, a TLR 4 agonist, triggers a variety of cellular responses that may have positive or negative effects on cellular activation downstream. In this study, the expression of TLR4 was investigated in untreated and LPS-treated THP-1 cells. THP-1 cells were cultured at a density of 2×10^5 cells/ml and incubated without and with different LPS concentrations (5, 10 & 20 ng/ml) for 24 hours. Total RNA was extracted and analysed for TLR4 expression using RT-PCR. It was observed that the expression of TLR4 in untreated THP-1 cells were overexpressed compared to the LPS-treated cells across all concentrations (Figure 3.1). This indicates that TLR4 is constitutively expressed in THP-1 cells. This is important for the study because THP-1 cells

were specifically chosen for this project as they are both innate immune and cancer cells. Upon stimulation by agonist such as LPS, innate immune cells reprogram their metabolism by displaying more dependence on glycolysis and reduced levels of OXPHOS – this is called the Warburg effect. Toll-like receptors (TLRs) are type I transmembrane proteins that have a leucine-rich repeat extracellular domain as well as a conserved Toll/Interleukin-1 (TIR) receptor domain in the cytoplasmic region (O'Neill *et al.*, 2003; Takeda and Akira, 2005). They are well known for their role in host defence against pathogens by recognising pathogen-associated molecular patterns (PAMPs) which are conserved molecular signatures (such as LPS) expressed by microbial pathogens (Henneke and Golenbock, 2002; Takeda *et al.*, 2002). Lipopolysaccharide is a component of the Gram-negative bacterial cell wall. In this study, LPS was used to mimic bacterial infection and it was observed that TLR 4 was also highly expressed at 5 ng/ml compared to other concentrations. This observation is consistent with the role of TLR4 in recognizing and defending cells against pathogens. Studies have shown that TLR mRNAs are strongly responsive to a variety of stimuli including infection, however, their expression may be significantly affected when activated by other TLR agonists (Flo *et al.*, 2001; Liu *et al.*, 2000). Another study showed that endotoxin protein-depleted LPS further increased the expression of many TLR mRNAs either than TLR 4. Interestingly, studies by Hirschfeld *et al.*, 2006 also showed that pre-treatment of THP-1 cells with PMA up-regulates the expression of TLR8 up to about 5-fold. TLR 8 expression has been shown to be further up-regulated by LPS to a final expression level 50 times that of untreated undifferentiated THP-1 cells and this may also explain the observed enhanced TLR 4 expression in untreated THP-1 cells. This may suggest that differentiating monocytes into macrophages might play a role in the level of TLR expression, therefore pre-treatment of THP-1 cells with PMA prior to treatment with LPS may have increased the expression of TLR4 during treatment with LPS compared to untreated cells.

This study has confirmed the expression of TLR4 in untreated THP-1 cells and LPS-treated cells, corroborating its role in immune defence.

4.2 Introduction of exogenous pyruvate or augmenting endogenous pyruvate induces apoptosis

It was expected that the THP-1 cells would be glycolytic since they are transformed cells. The impact of reversing the Warburg effect on cell proliferation was then tested. Thus, the cell cycle and the apoptotic effects of MP and DCA, were investigated in THP-1 cells. The cells were treated with various drugs in a time dependent manner and subsequently analysed using a flow cytometer. Cell cycle analysis revealed that treatment with MP resulted in an increase in cells at the Sub-G0 phase (Figure 3.2-3.6). This phase represents cells with fragmented DNA, which is a characteristic of cells undergoing apoptosis. This makes sense as MP and DCA target the unique cancer metabolism disrupting it therefore killing cells.

Apoptotic cell death was further measured by staining with Annexin V/PI stains (Figures 3.7 and 3.8). This study observed that when cells were treated with MP, only 8.0% increase in apoptosis was observed in comparison to untreated cells at only 2%.

DCA-treated cells also showed only 3.9% in apoptosis when compared to the untreated cells. DCA has been in use as a drug for treatment of lactic acidosis for decades and therefore details of the drug's pharmacokinetics and toxicity profile have been well studied (Stacpoole *et al.*, 1998). The studies by Bonnet *et al* (2007) showed that DCA has selective killing mechanisms that allows it to specifically target cancer cells and not normal cells. These selective mechanisms of inducing apoptosis include: depolarization of the mitochondrial membrane, suppression of glycolysis, production of reactive oxygen species, induction of the plasma membrane potassium channel, and release of pro-apoptotic factors from mitochondria. Wong *et al* (2008) showed that dichloroacetate caused apoptosis in endometrial cancer cells, while Cao *et al* (2008) showed that the DCA sensitized prostate cancer cells to radiation. In this study, 10 mM DCA was used to treat THP-1 cells and apoptosis was observed although only slightly. The slight apoptosis observed might be due to the concentration used as other studies have shown that a higher concentration of DCA (≥ 25 mM) induced increased apoptosis (Stockwin *et al.*, 2010; Madhok *et al.*, 2010; Xiao *et al.*, 2010; Heshu *et al.*, 2010;

Sun *et al.*, 2010). These findings suggest that by blocking the activity of pyruvate dehydrogenase kinase, leads to the activation of pyruvate dehydrogenase. DCA might be responsible for some of the observed apoptosis induction in THP-1 cells. Furthermore, most studies done utilized other cancer cell lines not THP-1 cells, thus the apoptotic effect of DCA might also be cancer specific. Other studies have also used DCA in combination with drugs such as Paclitaxel, therefore the effects of DCA as a sole drug might not have a significant effect in inducing apoptosis.

In this study, MP was found to be a better agent in inducing apoptosis of THP-1 cells even after stimulation of the TLR-4 signalling pathway by LPS as compared to DCA. Future studies using increased concentrations of DCA may prove important. Targeting the metabolism of cancer cells seem to be effective as shown in this study using MP.

4.3 Exogenous and endogenous pyruvate reverse the metabolic reprogramming in THP-1 cells (Warburg effect)

This study evaluated the impact of exogenous pyruvate and DCA on the metabolic programme of THP-1 cells. Furthermore, to establish the nature of the role played by TLR4. Cells were cultured in 96 well plates under previously mentioned conditions, and treated with different treatments for 24 hours. Cayman's dual assay (measures glycolysis and OXPHOS) kit was used to measure the metabolic pathways. It was established that THP-1 cells are already glycolytic. This study showed that introduction of exogenous MP reverses the Warburg effect by boosting OXPHOS even in the presence of LPS (stimulates TLR4) which according to literature, worsens the Warburg effect. In the first instance, this present study established that THP-1 cells were already glycolytic because glycolysis is elevated in untreated cells. Treatment of THP-1 cells with exogenous MP shifted the metabolism of cancer cells as it leads to significantly reduced glycolysis and higher OXPHOS (Figure 3.9-3.10). These findings suggest that exogenous MP indeed reverses the Warburg effect corroborating and confirming the hypothesis of a recent study by Monchusi and Ntwasa, 2017 that showed that exogenous MP kills cancer cells by evading the glycolytic pathway. MP is a lipophilic membrane permeable agent and when introduced exogenously it goes

directly into the TCA cycle, thereby boosting OXPHOS by inhibiting the Warburg effect (Lembert *et al.*, 2001). This study also observed no change in glycolysis and a slight increase in OXPHOS activity when THP-1 cells were treated with DCA (Figure 3.9, 3.10) indicating its role in reverse metabolic reprogramming. Endogenous DCA is an inhibitor of pyruvate dehydrogenase kinase (PDK), an enzyme that inhibits pyruvate dehydrogenase (PDH) which is responsible for catalysing the conversion of pyruvate into Acetyl CoA, which enters the tricarboxylic acid (TCA) cycle, and subsequently into OXPHOS. When PDK is active, it phosphorylates PDH, rendering it inactive and thus, reduces the entry of pyruvate into the TCA cycle. PDK plays an important role in promoting glycolysis and reducing levels of OXPHOS. Therefore, DCA inhibits PDK and consequently reduces glycolysis by boosting OXPHOS. However, in this study DCA did not reduce glycolysis but was able to increase OXPHOS, this may suggest that some of the pyruvate was still converted into lactate thus the increase in glycolysis (DCA acts endogenously). This study also mimicked infection in THP-1 cells by treatment with LPS. LPS treated cells did not show aggravated Warburg effect, since upon infection, innate immune cells rewire their metabolism in a manner similar to that observed in cancer cells. Treatment with MP and DCA boosted the OXPHOS pathway in LPS-treated cells further confirming their roles in reversing the Warburg effect

Although these drugs use different mechanisms, they both seem to target the metabolic program by either reducing glycolysis and/or increasing OXPHOS. Therefore, they might serve as possible therapeutic agents for cancer treatment.

4.4 Conclusion

Cancer cells prefer the less efficient glycolytic pathway (Warburg effect) as a source of energy production to enable proliferation. This preference is also observed during infection. This study has shown that indeed treatment with drugs such as MP and DCA drugs reprogram the metabolism of THP-1 cells resulting in cell death via apoptosis. Importantly, this study has observed that MP treatment was able to cause cell death by boosting OXPHOS and inhibiting the glycolytic

pathway. Taken together, targeting the energy metabolism of cancer cells provides a promising avenue for cancer therapy.

4.5 Future studies

Future studies corroborating the results observed in this study in *in vivo* models is crucial. Additionally, experiments comparing the effect of drugs such as MP and DCA in different cell lines should be performed. Furthermore, the molecular mechanisms involved in linking infection with cancer should also be investigated in various cell lines. Importantly, *in vivo* studies further confirming the effects of these drugs should be done.

REFERENCES

- Adrain, C. & Marti, S.J. (2001) The mitochondrial apoptosome: a killer unleashed by the cytochrome *seas*. *TiBS*. 26(6), 390-397.
- Akira S. and Takeda K. (2004). Toll-like receptor signalling. *Nat Rev Immunol*. 4, 499-511.
- Alenzi, F.Q. (2004). Links between apoptosis, proliferation and the cell cycle. *Br J Biomed Sci*. 61(2), 99-102.
- Badura S., Tesanovic T., Pfeifer H., Wystub S., Nijmeijer B.A., Liebermann M., Falkenburg J.H., Ruthardt M., Ottmann O.G. (2013). Differential effects of selective inhibitors targeting the PI3K/ AKT/mTOR pathway in acute lymphoblastic leukemia. *PLoS One*. 11: e80070.
- Balaban R.S., Nemoto S., Finkel T. (2005). Mitochondria, oxidants, and aging. *Cell* 120, 483---495.
- Balkwill, F. & Mantovani, A. (2001). Inflammation and cancer: back to Virchow *Lancet* 357, 539–545.
- Boneh A. (2006). Regulation Of mitochondrial oxidative phosphorylation by second messenger-mediated signal transduction mechanisms. *Cell Mol Life Sci* 63: 1236-1248.
- Bonnet, S., Archer, S.L., Allalunis-Turner, J., Haromy, A., Beaulieu, C., Thompson, R., Lee, C.T., Lopaschuk, G.D., Puttagunta, L., Bonnet, S., Harry, G., Hashimoto, K., Porter, C.J., Andrade, M.A., Thebaud, B., Michelakis, E.D. (2007). A mitochondria-K⁺ channel axis is suppressed in cancer and its normalization promotes apoptosis and inhibits cancer growth. *Cancer Cell*. 11, 37–51.
- Borrello, M. G. (2005). Induction of a proinflammatory program in normal human thyrocytes by the RET/PTC1 oncogene. *Proc. Natl Acad. Sci. USA*. 102, 14825–14830.
- Brown M. and Wittwer C. (2000). Flow cytometry: principles and clinical applications in hematology. *Clin Chem*. 46(8), 1221-1229.

Cleeter, M.W., Cooper, J.M., Darley-Usmar, V.M., Moncada, S., Schapira, A.H. (1994). Reversible inhibition of cytochrome c oxidase, the terminal enzyme of the mitochondrial respiratory chain, by nitric oxide. Implications for neurodegenerative diseases. *FEBS. Lett.* 345, 50-54.

Collins, K., Jacks, T., and Pavletich, N. P. 1997. The cell cycle and cancer. *Proc. Natl. Acad. Sci.* Vol 94, 2776–2778.

Collins T.J., Berridge M.J., Lipp P., Bootman M.D. (2002). Mitochondria Are morphologically and functionally heterogeneous within cells. *EMBO J* 21, 1616--1627.

Cooperstock M. (1974). Inactivation of endotoxin by Polymyxin B. *Antimicrob Agents Chemother.* 6, 4225.

Corfe, B. (2002) Suicide: A way of life. *The Biochemist*, pp. 9-11.

Corinti S, Albanesi C, la Sala A, Pastore S, Girolomoni G. (2001). Regulatory activity of autocrine IL-10 on dendritic cell functions. *J Immunol.* 166, 4312-8.

Creagh E.M., O'Neill L.A. (2006). TLRs, NLRs and RLRs: a trinity of pathogen sensors that cooperate in innate immunity. *Trends Immunol.* 27, 352-7.

Curtin, J.F., Liu, N., Candolfi, M., Xiong, W., Assi, H., Yagiz, K., Edwards, M.R., Michelsen, K.S., Kroeger, K.M., Liu, C., et al. (2009). HMGB1 Mediates Endogenous TLR2 Activation and Brain Tumor Regression. *PLoS Med* 6, e1000010.

Debatin K.M. (2004) Apoptosis pathways in cancer and cancer therapy. *Cancer Immunology Immunotherapy*, 53, 153-159.

DeBerardinis, R.J., Lum, J.J., Hatzivassiliou, G., and Thompson, C.B. (2008). The biology of cancer: Metabolic reprogramming fuels cell growth and proliferation. *Cell Metab.* 7, 11–20.

Denko, N.C. (2008). Hypoxia, HIF1 and glucose metabolism in the solid tumour. *Nat. Rev. Cancer.* 8, 705-713.

Drapier, J.C. and Hibbs, Jr J.B. (1988). Differentiation of murine macrophages to express nonspecific cytotoxicity for tumor cells results in L-arginine-dependent inhibition of mitochondrial iron-sulfur enzymes in the macrophage effector cells. *J. Immunol.* 140, 2829-2838.

Düfer, M., Krippeit-Drews, P., Buntinas, L., Siemen, D., and Drews, G. 2002. Methyl pyruvate stimulates pancreatic β -cells by a direct effect on KATP channels, and not as a mitochondrial substrate. *Biochem. J.* 368, 817-825.

Elstrom, R.L., Bauer, D.E., Buzzai, M., Karnauskas, R., Harris, M.H., Plas, D.R., Zhuang, H., Cinalli, R.M., Alavi, A., Rudin, C.M., et al. (2004). Akt stimulates aerobic glycolysis in cancer cells. *Cancer Res.* 64, 3892–3899.

Falagas E.M., Kasiakou S.K. (2005). The revival of polymyxins for the management of multidrug-resistant gram-negative bacterial infections. *Clin Infect Dis.* 40, 1333-41.

Flo T.H., Halaas O., Torp S., Ryan L., Lien E., Dybdahl B., Sundan A., Espevik T. (2001). Differential expression of Toll-like receptor 2 in human cells. *J Leukoc Biol.* 69(3):474-81.

Flossmann, E. & Rothwell, P. M. (2007). Effect of aspirin on long-term risk of colorectal cancer: consistent evidence from randomised and observational studies. *Lancet.* 369, 1603–1613.

Green, D.R. & Reed, J.C. (1998). Mitochondria and apoptosis. *Science.* 281, 1309-1312.

Golstein, P., Aubry, L. & Levraud, J. (2003) Cell-death alternative model organisms: why and which? *Nature Reviews: Mol. Cell Biology.* 4, 1- 10.

Henneke, P., and Golenbock, D.T. (2002). Innate immune recognition of lipopolysaccharide by endothelial cells. *Crit. Care Med.* 30, S207–S213.

Heshe, D., Hoogestraat, S., Brauckmann, C., Karst, U., Boos, J. and Lanvers-Kaminsky, C. (2011) Dichloroacetate Metabolically Targeted Therapy Defeats Cytotoxicity of Standard Anticancer Drugs. *Cancer Chemotherapy and Pharmacology*, 67, 647-655.

Himanshu K., Taro K. and Shizuo A. (2009). Toll-like receptors and innate immunity. *Biochemical and Biophysical research communications* 388, 621-625.

Hirschfeld, M., Weis, J. J., Toshchakov, V., Salkowski, C. A., Cody, M. J., Ward, D. C., Qureshi, N., Michalek, S. M. and Vogel, S. N. (2006). Signaling by toll-like receptor 2 and 4 agonists results in differential gene expression in murine macrophages. *Immun.* 69: 1477–1482.

Huang, B., Zhao, J., Li, H. (2005). Toll-like receptors on tumor cells facilitate evasion of immune surveillance. *Cancer Research.* 65:12, 5009–5014.

Haupt, S., et al., (2003). Apoptosis - the p53 network. *J Cell Sci.* 116, 4077-85.

INTERNATIONAL AGENCY FOR RESEARCH ON CANCER AND WORLD HEALTH ORGANIZATION. 2014. GLOBOCAN 2012: Estimated Cancer Incidence, Mortality and Prevalence Worldwide in 2012 [Online]. Available: http://globocan.iarc.fr/Pages/fact_sheets_population.aspx [Accessed 9 August 2017].

Ishiguro T, Ishiguro R, Ishiguro M, Iwai S. (2012). Co-treatment of dichloroacetate, omeprazole and tamoxifen exhibited synergistically antiproliferative effect on malignant tumors: in vivo experiments and a case report. *Hepato-gastroenterology*. 59, 994–996.

Israels, E.D. and L.G. Israels. (2000). The cell cycle. *Oncologist*. 5(6), 510-3.

Jacks, T. and Weinberg. 1998. The expanding role of cell cycle regulators. *Science*, vol 280, No 5366, 1035-1036.

Jantsch, J., Chakravorty, D., Turza, N., Prechtel, A.T., Buchholz, B., Gerlach, R.G., Volke, M., Gläsner, J., Warnecke, C., Wiesener, M.S., et al. (2008). Hypoxia and hypoxia-inducible factor-1 alpha modulate lipopolysaccharide-induced dendritic cell activation and function. *J. Immunol. Baltim. Md 1950* 180, 4697–4705.

Jin, S. and A.J. Levine. (2001). The p53 functional circuit. *J Cell Sci*. 114, 4139-40

Kato M, Li J, Chuang JL, Chuang DT. (2007). Distinct structural mechanisms for inhibition of pyruvate dehydrogenase kinase isoforms by AZD7545, dichloroacetate, and radicicol. *Structure*. 15, 992–1004.

Kaur, J. & Mohanti, B.K. (2011). Transition from Curative to Palliative Care in Cancer, In: *Indian Journal of Palliative Care*. [Online]. Available from: www.ncbi.nlm.nih.gov/pmc/pmc/articles/PMC3098537

Kerr J. F., Wyllie A. H., and Currie A. R. (1972) Apoptosis: a basic biological phenomenon with wide ranging implications in tissue kinetics. *Br J Cancer*, 26(4):239-257

Kim, J.W., Tchernyshyov, I., Semenza, G.L, Dang, C.V. (2006). HIF-1-mediated expression of pyruvate dehydrogenase kinase: a metabolic switch required for cellular adaptation to hypoxia. *Cell. Metab*. 3, 177–185.

Koehne, C. H. & Dubois, R. N. (2004). COX-2 inhibition and colorectal cancer. *Semin. Oncol*. 31, 12–21.

Kowaltowski A.J., De Souza-Pinto N.C., Castilho R.F., Vercesi A.E. (2009.) Mitochondria And reactive oxygen species. *Free Radic Biol Med* 47, 333---343.

Krawczyk, C.M., Holowka, T., Sun, J., Blagih, J., Amiel, E., DeBerardinis, R.J., Cross, J.R., Jung, E., Thompson, C.B., Jones, R. (2010). Toll-like receptor-induced changes in glycolytic metabolism regulate dendritic cell activation. *Blood* 115, 4742–4749.

Lemaitre B., Nicolas E., Michaut L., Reichhart J.M., Hoffmann J.A. (1996). The dorsoventral regulatory gene cassette spatzle/Toll/cactus controls the potent antifungal response in *Drosophila* adults. *Cell*. 86, 973-83.

Lembert, N., Joos, H.C., Idahl, L.A. et al. (2001). Methyl pyruvate initiates membrane depolarization and insulin release by metabolic factors other than ATP. *Biochem J*. 50, 345–354.

Liu AH. (2008). Innate microbial sensors and their relevance to allergy. *J Allergy Clin Immunol*. 122, 846-58.

Lorsbach R.B., Murphy W.J., Lowenstein C.J., Snyder S.H., Russell S.W. (1993). Expression of the nitric oxide synthase gene in mouse macrophages activated for tumour cell killing. *J Biol Chem*. 268, 1908-1913.

Madhok, B., Yeluri, S., Perry, S., Hughes, T. and Jayne, D. (2010) Dichloroacetate Induces Apoptosis and Cell-Cycle Arrest in Colorectal Cancer Cells. *British Journal of Cancer*, 102, 1746-1752.

Mardiros A., Brown C.E., Budde L.E., Wang X., Forman S.J. (2013). Acute myeloid leukemia therapeutics: CARs in the driver's seat. *Onco immunology*, 12: e27214.

Medzhitov R., Preston-Hurlburt P., Janeway C.A. Jr. (1997). A human homologue of the *Drosophila* Toll protein signals activation of adaptive immunity. *Nature*. 388, 394-7.

Michelakis, E.D., Webster, L., Mackey, J.R. (2008). Dichloroacetate (DCA) as a potential metabolitargeting therapy for cancer. *Br. J. Cancer* 99, 989–994.

Mole, D.R., Blancher, C., Copley, R.R. (2009). Genome-wide association of hypoxia-inducible factor (HIF)-1alpha and HIF-2alpha DNA binding with expression profiling of hypoxia-inducible transcripts. *Biol. Chem. J*. 284, 16767-16775.

Moyer J.H., Mills L.C., Yow E.M. (1953). Toxicity of polymyxin B. I. Animal studies with particular reference to evaluation of renal function. *Arch Intern Med*. 92, 238-47.

Monchusi, B., Ntwasa, M., 2017. Methyl pyruvate protects a normal lung fibroblast cell line from irinotecan-induced cell death: Potential use as adjunctive to chemotherapy. *PloS One* 12, e0182789.

Nigg, E. A. (1996). Cyclin-dependent kinase 7: at the cross-roads of transcription, DNA repair and cell cycle control. *Cell Biology*. 8, 312-317.

O'Neill, L.A.J., Fitzgerald, K.A., and Bowie, A.G. (2003). The Toll-IL-1 receptor adaptor family grows to five members. *Trends Immunol.* 24, 286–290.

Ouyang, L., Z. Shi, S. Zhao, F. T. Wang, T. T. Zhou, B. Liu & J. K. Bao (2012) Programmed cell death pathways in cancer: a review of apoptosis, autophagy and programmed necrosis. *Cell Prolif*, 45, 487-98.

Papandreou, I., Cairns, R.A., Fontana, L., Lim A.L., Denko N.C. (2006). HIF-1 mediates adaptation to hypoxia by actively downregulating mitochondrial oxygen consumption. *Cell. Metab.* 3,187-197.

Pardee, A.B. (1974). A restriction point for control of normal animal cell proliferation. *Proc. Natl. Acad. Sci.* 7, 1286–1290.

Park, M. T., and Lee, S. J. 2003. Cell cycle and cancer. *Journal of biochemistry and molecular cell biology*. Vol 36, no.1, 60-65.

Park, J.S., Gamboni-Robertson, F., He, Q., Svetkauskaite, D., Kim, J.-Y., Strassheim, D., Sohn, J.-W., Yamada, S., Maruyama, I., Banerjee, A., et al. (2006). High mobility group box 1 protein interacts with multiple Toll-like receptors. *Am. J. Physiol. Cell Physiol.* 290, C917–C924.

Parkin, D.M. (2006). The global health burden of infection-associated cancers in the year 2002. *Int. J. Cancer J. Int. Cancer* 118, 3030–3044.

Raucci, A., Palumbo, R., and Bianchi, M.E. (2007). HMGB1: A signal of necrosis. *Autoimmunity* 40, 285–289.

Raven, P.H. & Johnson, G.B. (1996), *Biology*, 4th ed., Wm. C. Brown Publishers, Dubuque.

Roach J.C., Glusman G., Rowen L., Kaur A., Purcell M.K., Smith K.D., Hood L.E., Aderem A. (2005). The evolution of vertebrate Toll-like receptors. *Proc Natl Acad Sci USA.* 102, 9577-82.

Rodríguez-Enríquez, S., Carreño-Fuentes, L., Gallardo-Pérez, J.C., Saavedra, E., Quezada, H., Vega, A., Marín-Hernández, A., Olín-Sandoval, V., Torres-Márquez, M.E., and Moreno-Sánchez, R. (2010). Oxidative phosphorylation is

impaired by prolonged hypoxia in breast and possibly in cervix carcinoma. *Int. J. Biochem. Cell Biol.* 42, 1744–1751.

Sag, D., Carling, D., Stout, R.D., Suttles, J. (2008). Adenosine 5'-monophosphate-activated protein kinase promotes macrophage polarization to an anti-inflammatory functional phenotype. *Immunol. J.* 181, 8633-8641.

Semenza, G.L., Neufelt, M.K., Chi, S.M., Antonarakis, S.E. (1991). Hypoxia-inducible nuclear factors bind to an enhancer element located 3' to the human erythropoietin gene. *Proc. Natl. Acad. Sci. USA.* 88, 5680-5684.

Semenza, G.L., Jiang, B.H., Leung, S.W. (1996). Hypoxia response elements in the aldolase A, enolase 1, and lactate dehydrogenase A gene promoters contain essential binding sites for hypoxia-inducible factor 1. *J Biol. Chem.* 271, 32529-32537.

Sherr C. J. (1996) Cancer cell cycles. *Science* 274:1672-77.

Sherr, C. J. (2000). The Pezcoller Lecture: Cancer Cell Cycles Revisited. *Cancer research*, 60, 3689–3695.

Shoji H. (2003). Extracorporeal endotoxin removal for the treatment of sepsis: endotoxin adsorption cartridge (Toraymyxin). *Ther Apher Dial.* 7, 108-14.

Stockwin L. H., Yu S. X., Borgel S., Hancock C., Wolfe T. L., Phillips L. R., Hollingshead M. G., Newton D. L. (2010). Sodium dichloroacetate selectively targets cells with defects in the mitochondrial ETC. *Int J Cancer*, 127(11):2510–2519.

Stacpoole P.W., Henderson G.N., Yan Z., Cornett R., James M.O. (1998). Pharmacokinetics, metabolism and toxicology of dichloroacetate. *Drug Metab Rev.* 30, 499–539.

Stacpoole P.W., Kurtz T.L., Han Z., Langaee T. (2008). Role of dichloroacetate in the treatment of genetic mitochondrial diseases. *Adv Drug Delivery Rev.* 60, 1478–1487.

Storm DR, Rosenthal KS, Swanson PE. (1977). Polymyxin and related peptide antibiotics. *Ann. Rev Biochem.* 46, 723-63.

Story, M. & Kodym, R. (1998) Signal transduction during apoptosis; implications for cancer therapy. *Frontiers in Bioscience*, 3, 365-375.

Sun R. C., Fadia M., Dahlstrom J. E., Parish C. R., Board P. G., Blackburn A. C. (2010). Reversal of the glycolytic phenotype by dichloroacetate inhibits

metastatic breast cancer cell growth in vitro and in vivo. *Breast Cancer Res Treat.* 120:253–260.

Takeda, K., Takeuchi, O., and Akira, S. (2002). Recognition of lipopeptides by Toll-like receptors. *J. Endotoxin. Res.* 8, 459–463.

Takeda, K., and Akira, S. (2004). TLR signaling pathways. *Semin. Immunol.* 16, 3–9.

Takeda, K., and Akira, S. (2005). Toll-like receptors in innate immunity. *Int. Immunol.* 17, 1–14.

Thornberry, N.A. & Lazebnik, Y. (1998) Caspases: Enemy within. *Science.* 281, 1312-1316.

Vardiman J.W., Thiele J., Arber D.A., Brunning R.D., Borowitz M.J., Porwit A., Harris N.L., Le Beau M.M., Hellström-Lindberg E., Tefferi A., Bloomfield C.D. (2009). The 2008 revision of the World Health Organization classification of myeloid neoplasms and acute leukemia: Rationale and important changes. *Blood.* 114, 937–51.

Vats D., Mukundan L., Odegaard J.I. (2006). Oxidative metabolism and PGC-1beta attenuate macrophage-mediated inflammation. *Cell Metab.* 4, 13-24.

Verhasselt V., Buelens C., Willems F., De Groote D., Haeffner-Cavaillon N., Goldman M. (1997). Bacterial lipopolysaccharide stimulates the production of cytokines and the expression of costimulatory molecules by human peripheral blood dendritic cells: evidence for a soluble CD14-dependent pathway. *J Immunol.* 158, 2919-25.

Vermes, I., Haanen, C. & Reutelingsperger, C.P.M. (1997) Apoptosis—the genetically controlled physiological cell death: biochemistry and measurement. *Ned. Tijdschr Klin. Chem.*, 22, pp. 43-50.

Vermeulen, K., D. R. Van Bockstaele & Z. N. Berneman (2003) The cell cycle: a review of regulation, deregulation and therapeutic targets in cancer. *Cell Prolif.* 36, 131-49.

Vincent J. L., Laterre P. F., Cohen J., Burchardi H., Bruining H., Lerma F.A. (2005). A pilot-controlled study of a polymyxin B-immobilized hemoperfusion cartridge in patients with severe sepsis secondary to intra-abdominal infection. 23, 400-5.

Vogelstein, B. and Kinzler, K.W. (2004). Cancer genes and the pathways they control. *Nat. Med.* 10, 789–799.

Warburg O., Wind F., Negelein E. (1927). The metabolism of tumors in the body. *J. Gen. Physiol.* 8, 519-530

- Warburg, O. (1956). On the origin of cancer cells. *Science* 123, 309–314.
- Wen, X., Lin X.Z., Liu B. and Wei Y.Q. (2012) Caspase-mediated programmed cell death pathways as potential therapeutic targets in cancer. *Cell Prolif*, 45, 217–224.
- West, A.P., Brodsky I.E., Rahner, C., Woo, D.K., Erdjument-Bromage, H., Tempst, P., Walsh, M.C., Choi, Y., Shadel, G.S., and Ghosh, S. (2011). TLR signalling augments macrophage bactericidal activity through mitochondrial ROS. *Nature* 472, 476–480.
- Wong, J.Y., Huggins, G.S., Debidda, M., Munshi, N.C., De Vivo, I. (2008). Dichloroacetate induces apoptosis in endometrial cancer cells. *Gynecol. Oncol.* 109, 394 –402.
- Xiao L., Li X., Niu N., Qian J., Xie G., Wang Y. (2010). Dichloroacetate (DCA) enhances tumor cell death in combination with oncolytic adenovirus armed with MDA-7/IL-24. *Molecular Cell Biochemistry.* 340, 31–40.
- Zhao Y, Liu H, Riker AI, Fodstad O, Ledoux SP, Wilson GL et al. (2011). Emerging metabolic targets in cancer therapy. *Front Biosci.* 16, 1844–1860.
- Zhao, T., Zhu, Y., Morinibu, A., Kobayashi, M., Shinomiya, K., Itasaka, S., Yoshimura, M., Guo, G., Hiraoka, M., and Harada, H. (2014). HIF-1-mediated metabolic reprogramming reduces ROS levels and facilitates the metastatic colonization of cancers in lungs. *Sci. Rep.* 4.
- Zughaier SM, Zimmer SM, Datta A, Carlson RW, Stephens DS. (2005). Differential induction of the toll-like receptor 4-MyD88-dependent and -independent signaling pathways by endotoxins. *Infect Immun.* 73, 2940-50.

APPENDIX A: CHEMICALS AND REAGENTS

Table A1: The following chemical and reagents were used in the study.

| Chemical/Reagent | Supplier | Catalogue no. |
|-------------------------------------|-------------------|----------------------|
| RPMI | Sigma | 13924 |
| Penicillin/Streptomycin | Sigma | P4333 |
| Fetal bovine serum (FBS) | Biowest | S181G |
| Dimethyl sulfoxide | Sigma | D8418 |
| Lipopolysaccharide | Sigma | L3024 |
| Sodium Dichloroacetate | Sigma | 347795 |
| Methyl pyruvate | Sigma | 37, 117-3 |
| Polymyxin B | Sigma | T3424-25ML |
| TRIZOL | Sigma | C-2432 |
| Chloroform | Sigma | 1036573 |
| Isopropanol | MERCK | UN 1170 |
| Ethanol absolute | VWR chemicals | 20821.330 |
| Nuclease free water | QIAGEN | 129117 |
| Ethidium Bromide | Sigma-Aldrich | 1239-45-8 |
| Agarose powder | White Sci. | 50004 |
| 1 kb Plus DNA ladder (0.1 µg/µl) | Thermo Scientific | SM1333 |
| 6X DNA loading dye | Thermo Scientific | R0611 |
| Glycerol | MERCK | 2676500LC |

APPENDIX B: LABORATORY EQUIPMENT

Table A2: The following laboratory equipment was used in this study.

| Equipment | Supplier and model no. |
|--------------------------------------|---------------------------------------|
| Vortex | Scientific industries 43178 |
| Heating block | Labnet D1100-230V |
| GeneAmp PCR machine | Perkin Elmer 2400 |
| Water bath | Julabo P 130 |
| Microscope | Olympus SZ40 |
| Microwave oven | KIC MWS- 900M |
| Weighing balance | Precisa XT220A |
| Labelling system | Bio-Rad XR+ |
| Orbit shaker | LAB-LINE 3521 3522-1 |
| Nano-drop spectrophotometer | Thermo-Fischer Scientific USA 1000 |
| Electrophoresis power supply | Bio-Rad 3000Xi |
| BD Accuri TM C6 cytometer | Biosciences BD Accuri C6+ |
| 4°C Refrigerator | KIC KBF 634/WH |

APPENDIX C: KITS

Table A3: The following kits were used in this study.

| Product name | Supplier | Catalogue number |
|--|-------------------|-------------------------|
| ProtoScript first strand cDNA synthesis kit | BioLabs Inc | E6300S; 0041411 |
| Taq 2x Master mix kit | BioLabs Inc | M0270L; 0231412 |
| Apoptosis kit | Thermo Scientific | BM 500FI-100 |
| Cell cycle kit | Thermo Scientific | F10797 |
| Oxygen Consumption/Glycolysis Dual assay kit | Cayman | 601060 |

APPENDIX D: BUFFERS

Table A4: The following buffers and composition were used in this study.

| Buffer | Composition |
|---------------------------|---|
| TAE buffer | 40mM Tris 20mM Acetic acid 1mM EDTA |
| Citric saline buffer 10X | 1.35 M KCL 0.15 M sodium azide |
| Phosphate buffered saline | Sigma (tablets) |

**APPENDIX E: CELL CYCLE RAW DATA GENERATED USING BD
ACCURI**

| <i>Cell cycle</i> | |
|--|-----------------------|
| Plot 4: A02 Untreated stained: Gated on (Singlets in all) and (P2 in all) | % of This Plot |
| This Plot | 100,00% |
| G0/G1 (296,429.0 / 499,404.0) | 53,47% |
| S phase (499,405.0 / 702,381.0) | 18,04% |
| G2/M (702,382.0 / 944,643.0) | 19,31% |
| Dead (100,000.0 / 302,975.0) | 4,46% |
| | |
| Plot 4: A03 Untreated stained 2: Gated on (Singlets in all) and (P2 in all) | % of This Plot |
| This Plot | 100,00% |
| G0/G1 (296,429.0 / 499,404.0) | 51,39% |
| S phase (499,405.0 / 702,381.0) | 18,89% |
| G2/M (702,382.0 / 944,643.0) | 19,41% |
| Dead (100,000.0 / 302,975.0) | 5,32% |
| | |
| Plot 4: A04 Untreated stained 3: Gated on (Singlets in all) and (P2 in all) | % of This Plot |
| This Plot | 100,00% |
| G0/G1 (296,429.0 / 499,404.0) | 53,09% |
| S phase (499,405.0 / 702,381.0) | 17,90% |
| G2/M (702,382.0 / 944,643.0) | 18,85% |
| Dead (100,000.0 / 302,975.0) | 4,82% |
| | |
| Plot 4: A05 LPS1: Gated on (Singlets in all) and (P2 in all) | % of This Plot |
| This Plot | 100,00% |
| G0/G1 (296,429.0 / 499,404.0) | 52,21% |
| S phase (499,405.0 / 702,381.0) | 20,35% |
| G2/M (702,382.0 / 944,643.0) | 14,22% |
| Dead (100,000.0 / 302,975.0) | 8,33% |
| | |
| Plot 4: A06 LPS2: Gated on (Singlets in all) and (P2 in all) | % of This Plot |
| This Plot | 100,00% |
| G0/G1 (296,429.0 / 499,404.0) | 52,51% |
| S phase (499,405.0 / 702,381.0) | 18,59% |
| G2/M (702,382.0 / 944,643.0) | 19,12% |
| Dead (100,000.0 / 302,975.0) | 4,01% |
| | |

| | |
|---|-----------------------|
| Plot 4: A07 LPS3: Gated on (Singlets in all) and (P2 in all) | % of This Plot |
| This Plot | 100,00% |
| G0/G1 (296,429.0 / 499,404.0) | 52,25% |
| S phase (499,405.0 / 702,381.0) | 19,76% |
| G2/M (702,382.0 / 944,643.0) | 18,44% |
| Dead (100,000.0 / 302,975.0) | 4,53% |
| | |
| Plot 4: A08 MP1: Gated on (Singlets in all) and (P2 in all) | % of This Plot |
| This Plot | 100,00% |
| G0/G1 (296,429.0 / 499,404.0) | 52,93% |
| S phase (499,405.0 / 702,381.0) | 19,21% |
| G2/M (702,382.0 / 944,643.0) | 16,71% |
| Dead (100,000.0 / 302,975.0) | 5,53% |
| | |
| Plot 4: A09 MP2: Gated on (Singlets in all) and (P2 in all) | % of This Plot |
| This Plot | 100,00% |
| G0/G1 (296,429.0 / 499,404.0) | 54,37% |
| S phase (499,405.0 / 702,381.0) | 19,84% |
| G2/M (702,382.0 / 944,643.0) | 17,51% |
| Dead (100,000.0 / 302,975.0) | 3,89% |
| | |
| Plot 4: A10 MP3: Gated on (Singlets in all) and (P2 in all) | % of This Plot |
| This Plot | 100,00% |
| G0/G1 (296,429.0 / 499,404.0) | 53,86% |
| S phase (499,405.0 / 702,381.0) | 17,99% |
| G2/M (702,382.0 / 944,643.0) | 16,52% |
| Dead (100,000.0 / 302,975.0) | 5,62% |
| | |
| Plot 4: A11 DCA1: Gated on (Singlets in all) and (P2 in all) | % of This Plot |
| This Plot | 100,00% |
| G0/G1 (296,429.0 / 499,404.0) | 52,52% |
| S phase (499,405.0 / 702,381.0) | 19,23% |
| G2/M (702,382.0 / 944,643.0) | 18,14% |
| Dead (100,000.0 / 302,975.0) | 5,48% |
| | |
| Plot 4: A12 DCA2: Gated on (Singlets in all) and (P2 in all) | % of This Plot |
| This Plot | 100,00% |
| G0/G1 (296,429.0 / 499,404.0) | 53,36% |

| | |
|---|-----------------------|
| S phase (499,405.0 / 702,381.0) | 19,68% |
| G2/M (702,382.0 / 944,643.0) | 13,53% |
| Dead (100,000.0 / 302,975.0) | 8,63% |
| | |
| Plot 4: B01 DCA3: Gated on (Singlets in all) and (P2 in all) | % of This Plot |
| This Plot | 100,00% |
| G0/G1 (296,429.0 / 499,404.0) | 52,47% |
| S phase (499,405.0 / 702,381.0) | 19,39% |
| G2/M (702,382.0 / 944,643.0) | 18,56% |
| Dead (100,000.0 / 302,975.0) | 4,32% |
| | |
| Plot 4: B02 PmB1: Gated on (Singlets in all) and (P2 in all) | % of This Plot |
| This Plot | 100,00% |
| G0/G1 (296,429.0 / 499,404.0) | 54,51% |
| S phase (499,405.0 / 702,381.0) | 20,78% |
| G2/M (702,382.0 / 944,643.0) | 14,48% |
| Dead (100,000.0 / 302,975.0) | 5,39% |
| | |
| Plot 4: B03 PmB2: Gated on (Singlets in all) and (P2 in all) | % of This Plot |
| This Plot | 100,00% |
| G0/G1 (296,429.0 / 499,404.0) | 55,36% |
| S phase (499,405.0 / 702,381.0) | 19,59% |
| G2/M (702,382.0 / 944,643.0) | 15,08% |
| Dead (100,000.0 / 302,975.0) | 4,96% |
| | |
| Plot 4: B04 PmB3: Gated on (Singlets in all) and (P2 in all) | % of This Plot |
| This Plot | 100,00% |
| G0/G1 (296,429.0 / 499,404.0) | 55,39% |
| S phase (499,405.0 / 702,381.0) | 19,28% |
| G2/M (702,382.0 / 944,643.0) | 15,34% |
| Dead (100,000.0 / 302,975.0) | 4,53% |
| | |
| Plot 4: B05 LPS +MP1: Gated on (Singlets in all) and (P2 in all) | % of This Plot |
| This Plot | 100,00% |
| G0/G1 (296,429.0 / 499,404.0) | 51,91% |
| S phase (499,405.0 / 702,381.0) | 19,47% |
| G2/M (702,382.0 / 944,643.0) | 17,25% |
| Dead (100,000.0 / 302,975.0) | 4,58% |

| | |
|---|-----------------------|
| | |
| Plot 4: B06 LPS +MP2: Gated on (Singlets in all) and (P2 in all) | % of This Plot |
| This Plot | 100,00% |
| G0/G1 (296,429.0 / 499,404.0) | 53,02% |
| S phase (499,405.0 / 702,381.0) | 19,48% |
| G2/M (702,382.0 / 944,643.0) | 15,45% |
| Dead (100,000.0 / 302,975.0) | 4,85% |
| | |
| Plot 4: B07 LPS +MP3: Gated on (Singlets in all) and (P2 in all) | % of This Plot |
| This Plot | 100,00% |
| G0/G1 (296,429.0 / 499,404.0) | 53,62% |
| S phase (499,405.0 / 702,381.0) | 18,23% |
| G2/M (702,382.0 / 944,643.0) | 14,22% |
| Dead (100,000.0 / 302,975.0) | 5,55% |
| | |
| Plot 4: B08 LPS +DCA1: Gated on (Singlets in all) and (P2 in all) | % of This Plot |
| This Plot | 100,00% |
| G0/G1 (296,429.0 / 499,404.0) | 50,16% |
| S phase (499,405.0 / 702,381.0) | 18,78% |
| G2/M (702,382.0 / 944,643.0) | 20,33% |
| Dead (100,000.0 / 302,975.0) | 4,16% |
| | |
| Plot 4: B09 LPS +DCA2: Gated on (Singlets in all) and (P2 in all) | % of This Plot |
| This Plot | 100,00% |
| G0/G1 (296,429.0 / 499,404.0) | 48,86% |
| S phase (499,405.0 / 702,381.0) | 17,91% |
| G2/M (702,382.0 / 944,643.0) | 18,79% |
| Dead (100,000.0 / 302,975.0) | 4,56% |
| | |
| Plot 4: B10 LPS +DCA3: Gated on (Singlets in all) and (P2 in all) | % of This Plot |
| This Plot | 100,00% |
| G0/G1 (296,429.0 / 499,404.0) | 48,05% |
| S phase (499,405.0 / 702,381.0) | 19,57% |
| G2/M (702,382.0 / 944,643.0) | 20,95% |
| Dead (100,000.0 / 302,975.0) | 4,82% |
| | |
| Plot 4: B11 LPS +PmB 1: Gated on (Singlets in all) and (P2 in all) | % of This Plot |
| This Plot | 100,00% |

| | |
|--|-----------------------|
| G0/G1 (296,429.0 / 499,404.0) | 52,44% |
| S phase (499,405.0 / 702,381.0) | 25,40% |
| G2/M (702,382.0 / 944,643.0) | 2,88% |
| Dead (100,000.0 / 302,975.0) | 17,76% |
| | |
| Plot 4: B12 LPS +PmB2: Gated on (Singlets in all) and (P2 in all) | % of This Plot |
| This Plot | 100,00% |
| G0/G1 (296,429.0 / 499,404.0) | 55,02% |
| S phase (499,405.0 / 702,381.0) | 20,15% |
| G2/M (702,382.0 / 944,643.0) | 16,01% |
| Dead (100,000.0 / 302,975.0) | 4,85% |
| | |
| Plot 4: C01 lps+mp+pMb: Gated on (Singlets in all) and (P2 in all) | % of This Plot |
| This Plot | 100,00% |
| G0/G1 (296,429.0 / 499,404.0) | 54,11% |
| S phase (499,405.0 / 702,381.0) | 20,57% |
| G2/M (702,382.0 / 944,643.0) | 14,39% |
| Dead (100,000.0 / 302,975.0) | 3,71% |
| | |
| Plot 4: C02 LPS+MP+PmB 2: Gated on (Singlets in all) and (P2 in all) | % of This Plot |
| This Plot | 100,00% |
| G0/G1 (296,429.0 / 499,404.0) | 51,64% |
| S phase (499,405.0 / 702,381.0) | 18,46% |
| G2/M (702,382.0 / 944,643.0) | 16,82% |
| Dead (100,000.0 / 302,975.0) | 4,75% |
| | |
| Plot 4: C03 LPS+DCA+PmB 1: Gated on (Singlets in all) and (P2 in all) | % of This Plot |
| This Plot | 100,00% |
| G0/G1 (296,429.0 / 499,404.0) | 53,93% |
| S phase (499,405.0 / 702,381.0) | 20,50% |
| G2/M (702,382.0 / 944,643.0) | 15,25% |
| Dead (100,000.0 / 302,975.0) | 4,04% |
| | |
| Plot 4: C04 LPS+MP+PmB 3: Gated on (Singlets in all) and (P2 in all) | % of This Plot |
| This Plot | 100,00% |
| G0/G1 (296,429.0 / 499,404.0) | 52,70% |
| S phase (499,405.0 / 702,381.0) | 19,16% |
| G2/M (702,382.0 / 944,643.0) | 15,07% |
| Dead (100,000.0 / 302,975.0) | 4,28% |

| | |
|--|-----------------------|
| Plot 4: C05 LPS+DCA+PmB 2: Gated on (Singlets in all) and (P2 in all) | % of This Plot |
| This Plot | 100,00% |
| G0/G1 (296,429.0 / 499,404.0) | 51,85% |
| S phase (499,405.0 / 702,381.0) | 20,17% |
| G2/M (702,382.0 / 944,643.0) | 16,07% |
| Dead (100,000.0 / 302,975.0) | 4,78% |
| | |
| Plot 4: C06 LPS+DCA+PmB 3: Gated on (Singlets in all) and (P2 in all) | % of This Plot |
| This Plot | 100,00% |
| G0/G1 (296,429.0 / 499,404.0) | 50,88% |
| S phase (499,405.0 / 702,381.0) | 17,92% |
| G2/M (702,382.0 / 944,643.0) | 17,43% |
| Dead (100,000.0 / 302,975.0) | 5,84% |
| | |
| Plot 4: C07 IR8mM: Gated on (Singlets in all) and (P2 in all) | % of This Plot |
| This Plot | 100,00% |
| G0/G1 (296,429.0 / 499,404.0) | 65,31% |
| S phase (499,405.0 / 702,381.0) | 11,26% |
| G2/M (702,382.0 / 944,643.0) | 6,45% |
| Dead (100,000.0 / 302,975.0) | 13,10% |
| | |
| Plot 4: C12 LPS +PmB3: Gated on (Singlets in all) and (P2 in all) | % of This Plot |
| This Plot | 100,00% |
| G0/G1 (296,429.0 / 499,404.0) | 46,82% |
| S phase (499,405.0 / 702,381.0) | 21,98% |
| G2/M (702,382.0 / 944,643.0) | 18,41% |
| Dead (100,000.0 / 302,975.0) | 6,07% |

**APPENDIX F: FLOW CYTOMETRY OBTAINED APOPTOSIS
RESULTS, FOLLOWING VARIOUS TREATMENTS**

| <i>Apoptosis</i> | |
|---|-----------------------|
| Plot 2: A01 Untreated UNstained: Gated on (Cells in all) | % of This Plot |
| This Plot | 100,00% |
| Necrotic | 0,03% |
| Late Apop | 0,00% |
| Live cells | 99,97% |
| Early Apop | 0,00% |
| | |
| Plot 2: A02 Annexin V only: Gated on (Cells in all) | % of This Plot |
| This Plot | 100,00% |
| Necrotic | 0,03% |
| Late Apop | 0,18% |
| Live cells | 97,27% |
| Early Apop | 2,52% |
| | |
| Plot 2: A03 PI only: Gated on (Cells in all) | % of This Plot |
| This Plot | 100,00% |
| Necrotic | 2,76% |
| Late Apop | 0,00% |
| Live cells | 97,24% |
| Early Apop | 0,00% |
| | |
| Plot 2: A04 untreated stained: Gated on (Cells in all) | % of This Plot |
| This Plot | 100,00% |
| Necrotic | 0,84% |
| Late Apop | 2,44% |
| Live cells | 96,24% |
| Early Apop | 0,47% |
| | |
| Plot 2: A05 US: Gated on (Cells in all) | % of This Plot |
| This Plot | 100,00% |
| Necrotic | 0,94% |
| Late Apop | 2,35% |
| Live cells | 96,35% |
| Early Apop | 0,36% |
| | |
| Plot 2: A06 US2: Gated on (Cells in all) | % of This Plot |
| This Plot | 100,00% |
| Necrotic | 1,08% |
| Late Apop | 2,40% |

| | |
|---|-----------------------|
| Live cells | 96,23% |
| Early Apop | 0,29% |
| | |
| Plot 2: A07 LPS 1: Gated on (Cells in all) | % of This Plot |
| This Plot | 100,00% |
| Necrotic | 1,99% |
| Late Apop | 3,38% |
| Live cells | 94,28% |
| Early Apop | 0,35% |
| | |
| Plot 2: A08 LPS 2: Gated on (Cells in all) | % of This Plot |
| This Plot | 100,00% |
| Necrotic | 2,09% |
| Late Apop | 2,73% |
| Live cells | 94,82% |
| Early Apop | 0,35% |
| | |
| Plot 2: A09 LPS 3: Gated on (Cells in all) | % of This Plot |
| This Plot | 100,00% |
| Necrotic | 2,02% |
| Late Apop | 2,93% |
| Live cells | 94,72% |
| Early Apop | 0,33% |
| | |
| Plot 2: A10 LPS+DCA: Gated on (Cells in all) | % of This Plot |
| This Plot | 100,00% |
| Necrotic | 1,81% |
| Late Apop | 4,05% |
| Live cells | 93,85% |
| Early Apop | 0,30% |
| | |
| Plot 2: A11 LPS+DCA 2: Gated on (Cells in all) | % of This Plot |
| This Plot | 100,00% |
| Necrotic | 1,15% |
| Late Apop | 5,24% |
| Live cells | 93,31% |
| Early Apop | 0,30% |
| | |
| Plot 2: A12 LPS+DCA 3: Gated on (Cells in all) | % of This Plot |
| This Plot | 100,00% |
| Necrotic | 1,52% |
| Late Apop | 3,98% |

| | |
|---|-----------------------|
| Live cells | 94,11% |
| Early Apop | 0,39% |
| | |
| Plot 2: B01 LPS+MP: Gated on (Cells in all) | % of This Plot |
| This Plot | 100,00% |
| Necrotic | 1,37% |
| Late Apop | 2,53% |
| Live cells | 95,72% |
| Early Apop | 0,38% |
| | |
| Plot 2: B02 LPS+MP2: Gated on (Cells in all) | % of This Plot |
| This Plot | 100,00% |
| Necrotic | 2,91% |
| Late Apop | 6,06% |
| Live cells | 90,60% |
| Early Apop | 0,43% |
| | |
| Plot 2: B03 LPS+MP3: Gated on (Cells in all) | % of This Plot |
| This Plot | 100,00% |
| Necrotic | 1,93% |
| Late Apop | 6,67% |
| Live cells | 90,76% |
| Early Apop | 0,65% |
| | |
| Plot 2: B04 LPS+PmB: Gated on (Cells in all) | % of This Plot |
| This Plot | 100,00% |
| Necrotic | 1,38% |
| Late Apop | 2,96% |
| Live cells | 95,34% |
| Early Apop | 0,33% |
| | |
| Plot 2: B05 LPS+PmB 2: Gated on (Cells in all) | % of This Plot |
| This Plot | 100,00% |
| Necrotic | 1,11% |
| Late Apop | 5,90% |
| Live cells | 92,34% |
| Early Apop | 0,65% |
| | |
| Plot 2: B06 LPS+PmB: Gated on (Cells in all) | % of This Plot |
| This Plot | 100,00% |
| Necrotic | 0,72% |
| Late Apop | 2,70% |

| | |
|---|-----------------------|
| Live cells | 96,11% |
| Early Apop | 0,47% |
| | |
| Plot 2: B07 LPS+PmB+DCA: Gated on (Cells in all) | % of This Plot |
| This Plot | 100,00% |
| Necrotic | 1,19% |
| Late Apop | 3,88% |
| Live cells | 94,53% |
| Early Apop | 0,39% |
| | |
| Plot 2: B08 LPS+PmB+DCA 2: Gated on (Cells in all) | % of This Plot |
| This Plot | 100,00% |
| Necrotic | 1,50% |
| Late Apop | 6,13% |
| Live cells | 91,60% |
| Early Apop | 0,78% |
| | |
| Plot 2: B09 LPS+PmB+DCA 3: Gated on (Cells in all) | % of This Plot |
| This Plot | 100,00% |
| Necrotic | 0,73% |
| Late Apop | 3,48% |
| Live cells | 95,16% |
| Early Apop | 0,64% |
| | |
| Plot 2: B10 LPS+PmB+MP: Gated on (Cells in all) | % of This Plot |
| This Plot | 100,00% |
| Necrotic | 0,88% |
| Late Apop | 3,81% |
| Live cells | 94,80% |
| Early Apop | 0,51% |
| | |
| Plot 2: B11 LPS+PmB+MP 2: Gated on (Cells in all) | % of This Plot |
| This Plot | 100,00% |
| Necrotic | 1,47% |
| Late Apop | 4,93% |
| Live cells | 92,88% |
| Early Apop | 0,73% |
| | |
| Plot 2: B12 LPS+PmB+MP 3: Gated on (Cells in all) | % of This Plot |
| This Plot | 100,00% |
| Necrotic | 1,28% |
| Late Apop | 4,15% |

| | |
|--|-----------------------|
| Live cells | 94,06% |
| Early Apop | 0,51% |
| | |
| Plot 2: C01 IR 8uM: Gated on (Cells in all) | % of This Plot |
| This Plot | 100,00% |
| Necrotic | 33,35% |
| Late Apop | 12,22% |
| Live cells | 52,09% |
| Early Apop | 2,34% |
| | |
| Plot 2: C02 PmB: Gated on (Cells in all) | % of This Plot |
| This Plot | 100,00% |
| Necrotic | 1,31% |
| Late Apop | 2,67% |
| Live cells | 95,74% |
| Early Apop | 0,28% |
| | |
| Plot 2: C03 PmB 2: Gated on (Cells in all) | % of This Plot |
| This Plot | 100,00% |
| Necrotic | 1,27% |
| Late Apop | 2,63% |
| Live cells | 95,85% |
| Early Apop | 0,26% |
| | |
| Plot 2: C04 PmB 3: Gated on (Cells in all) | % of This Plot |
| This Plot | 100,00% |
| Necrotic | 1,04% |
| Late Apop | 2,73% |
| Live cells | 95,86% |
| Early Apop | 0,36% |
| | |
| Plot 2: C05 MP: Gated on (Cells in all) | % of This Plot |
| This Plot | 100,00% |
| Necrotic | 2,64% |
| Late Apop | 6,38% |
| Live cells | 90,26% |
| Early Apop | 0,72% |
| | |
| Plot 2: C06 MP2: Gated on (Cells in all) | % of This Plot |
| This Plot | 100,00% |
| Necrotic | 1,32% |
| Late Apop | 7,99% |

| | |
|---|-----------------------|
| Live cells | 89,52% |
| Early Apop | 1,17% |
| | |
| Plot 2: C07 MP3: Gated on (Cells in all) | % of This Plot |
| This Plot | 100,00% |
| Necrotic | 1,65% |
| Late Apop | 6,45% |
| Live cells | 90,85% |
| Early Apop | 1,05% |
| | |
| Plot 2: C08 DCA: Gated on (Cells in all) | % of This Plot |
| This Plot | 100,00% |
| Necrotic | 0,42% |
| Late Apop | 3,90% |
| Live cells | 94,72% |
| Early Apop | 0,96% |
| | |
| Plot 2: C09 DCA2: Gated on (Cells in all) | % of This Plot |
| This Plot | 100,00% |
| Necrotic | 1,09% |
| Late Apop | 3,23% |
| Live cells | 95,07% |
| Early Apop | 0,61% |
| | |
| Plot 2: C10 DCA 3: Gated on (Cells in all) | % of This Plot |
| This Plot | 100,00% |
| Necrotic | 0,59% |
| Late Apop | 3,43% |
| Live cells | 95,55% |
| Early Apop | 0,44% |

APPENDIX G: GLYCOLYSIS RESULTS AND STANDARD CURVE
FOLLOWING 24 HOURS OF TREATMENT

| Glycolysis | | | | | | | |
|---------------|-------------|-------------|-------------|-------------|-------------|-------------|-------------|
| Photometric 1 | | | | | | | |
| Plate 1: 1 | | | | | | | |
| Sample | 1 | 2 | 3 | 4 | 5 | 6 | 7 |
| A | Un_0001 1/1 | Un_0009 1/1 | Un_0017 1/1 | Un_0025 1/1 | Un_0033 1/1 | Un_0041 1/1 | Un_0049 1/1 |
| B | Un_0002 1/1 | Un_0010 1/1 | Un_0018 1/1 | Un_0026 1/1 | Un_0034 1/1 | Un_0042 1/1 | Un_0050 1/1 |
| C | Un_0003 1/1 | Un_0011 1/1 | Un_0019 1/1 | Un_0027 1/1 | | | |
| D | Un_0004 1/1 | Un_0012 1/1 | Un_0020 1/1 | Un_0028 1/1 | | | |
| E | Un_0005 1/1 | Un_0013 1/1 | Un_0021 1/1 | Un_0029 1/1 | | | |
| F | Un_0006 1/1 | Un_0014 1/1 | Un_0022 1/1 | Un_0030 1/1 | | | |
| G | Un_0007 1/1 | Un_0015 1/1 | Un_0023 1/1 | Un_0031 1/1 | | | |
| H | Un_0008 1/1 | Un_0016 1/1 | Un_0024 1/1 | Un_0032 1/1 | | | |
| Value | 1 | 2 | 3 | 4 | 5 | 6 | 7 |
| A | 1,34749 | 0,762324 | 0,757559 | 0,742162 | 0,565702 | 0,687439 | 0,671598 |
| B | 0,969794 | 0,689416 | 0,697977 | 0,710572 | 0,627537 | 0,559661 | 0,667925 |
| C | 0,634989 | 0,420753 | 0,30401 | 0,420631 | | | |
| D | 0,470702 | 0,525211 | 0,526493 | 0,488633 | | | |
| E | 0,339059 | 0,576554 | 0,417065 | 0,462494 | | | |
| F | 0,227861 | 0,474873 | 0,485556 | 0,483083 | | | |
| G | 0,32476 | 0,519274 | 0,709237 | 0,604653 | | | |
| H | 0,305143 | 0,628005 | 0,638235 | 0,611113 | | | |

L-Lactate Standard Curve

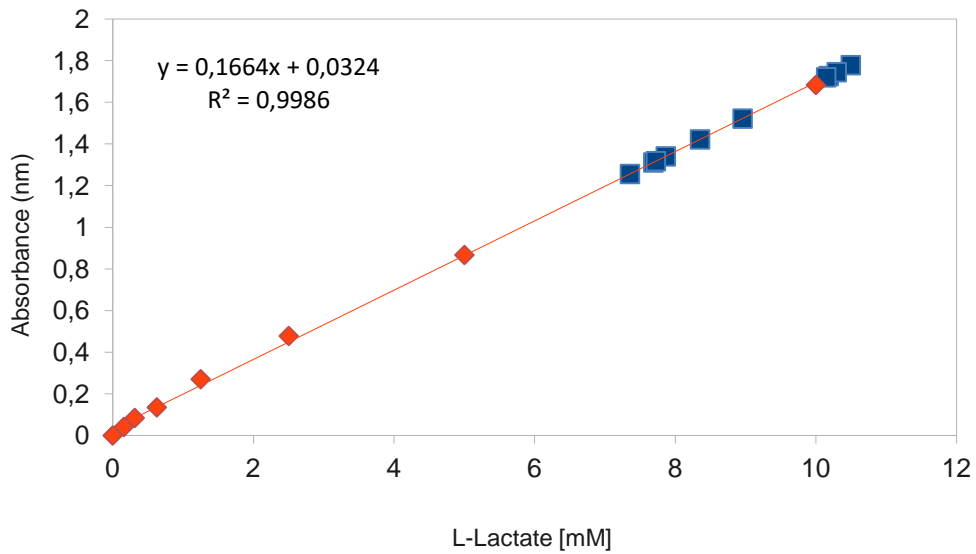


Figure A1: Standard curve for the L-Lactate concentrations obtained from the L-lactate concentrations (orange) and glycolysis assay treatments (blue). The values were generated from the plate reader and exported to excel for standard curve generation.

APPENDIX H: OXPLOS RESULTS FOLLOWING 24 HOURS OF TREATMENT

| Sample | 1 | 2 | 3 | 4 | 5 | 6 | 7 |
|------------------------------|----------------|----------------|----------------|----------------|----------------|----------------|----------------|
| A | Un_0001 1/1 | Un_0009 1/1 | Un_0017 1/1 | Un_0025 1/1 | Un_0033 1/1 | Un_0041 1/1 | |
| B | Un_0002 1/1 | Un_0010 1/1 | Un_0018 1/1 | Un_0026 1/1 | Un_0034 1/1 | Un_0042 1/1 | |
| C | Un_0003 1/1 | Un_0011 1/1 | Un_0019 1/1 | Un_0027 1/1 | Un_0035 1/1 | Un_0043 1/1 | |
| D | Un_0004 1/1 | Un_0012 1/1 | Un_0020 1/1 | | | | |
| E | Un_0005 1/1 | Un_0013 1/1 | Un_0021 1/1 | | | | |
| F | Un_0006 1/1 | Un_0014 1/1 | Un_0022 1/1 | | | | |
| G | Un_0007 1/1 | Un_0015 1/1 | Un_0023 1/1 | | | | |
| H | Un_0008 1/1 | Un_0016 1/1 | Un_0024 1/1 | Un_0032 1/1 | Un_0040 1/1 | Un_0048 1/1 | Un_0056 1/1 |
| | | | | | | | |
| Value | 1 | 2 | 3 | 4 | 5 | 6 | 7 |
| A | 126,184 | 124,694 | 120,026 | 121,404 | 113,083 | 118,559 | |
| B | 110,921 | 123,525 | 132,809 | 102,081 | 103,021 | 114,38 | |
| C | 127,515 | 132,707 | 130,075 | 115,299 | 112,946 | 107,334 | |
| D | 127,085 | 132,395 | 141,782 | | | | |
| E | 94,8322 | 124,022 | 119,39 | | | | |
| F | 142,093 | 125,162 | 117,615 | | | | |
| G | 148,753 | 187,122 | 117,667 | | | | |
| H | 1,53055 | 0,91387 | 0,87085 | 110,69 | 103,315 | 97,2942 | 91,0147 |
| Plate 1: 1, reading 2 | | | | | | | |
| Sample | 1 | 2 | 3 | 4 | 5 | 6 | 7 |
| A | Un_0001 1/1 | Un_0009 1/1 | Un_0017 1/1 | Un_0025 1/1 | Un_0033 1/1 | Un_0041 1/1 | |
| B | Un_0002 1/1 | Un_0010 1/1 | Un_0018 1/1 | Un_0026 1/1 | Un_0034 1/1 | Un_0042 1/1 | |
| C | Un_0003 1/1 | Un_0011 1/1 | Un_0019 1/1 | Un_0027 1/1 | Un_0035 1/1 | Un_0043 1/1 | |
| D | Un_0004 1/1 | Un_0012 1/1 | Un_0020 1/1 | | | | |
| E | Un_0005 1/1 | Un_0013 1/1 | Un_0021 1/1 | | | | |

| | | | | | | | |
|--------------|----------------|----------------|----------------|----------------|----------------|----------------|----------------|
| F | Un_0006 1/1 | Un_0014 1/1 | Un_0022 1/1 | | | | |
| G | Un_0007 1/1 | Un_0015 1/1 | Un_0023 1/1 | | | | |
| H | Un_0008 1/1 | Un_0016 1/1 | Un_0024 1/1 | Un_0032 1/1 | Un_0040 1/1 | Un_0048 1/1 | Un_0056 1/1 |
| Value | 1 | 2 | 3 | 4 | 5 | 6 | 7 |
| A | 106,121 | 111,388 | 105,627 | 109,687 | 101,446 | 110,285 | |
| B | 98,2672 | 96,7918 | 105,3 | 87,9782 | 88,1424 | 99,1632 | |
| C | 112,737 | 102,999 | 109,259 | 100,592 | 95,4129 | 96,2257 | |
| D | 113,842 | 92,4084 | 120,719 | | | | |
| E | 83,5254 | 90,0705 | 108,628 | | | | |
| F | 122,359 | 104,235 | 104,34 | | | | |
| G | 130,704 | 166,306 | 102,846 | | | | |
| H | 0,58926 | 1,08193 | 0,2357 | 99,3138 | 100,573 | 91,5644 | 85,6803 |